NBSIR 73-316
(AFAPL-TR-73-72)

LIQUID HELIUM PUMPS

Philip M. McConnell

Cryogenics Division
Institute for Basic Standards
National Bureau of Standards
Boulder, Colorado 80302

Interim Report

June 1973

NBSIR 73-316
(AFAPL-TR-73-72)

LIQUID HELIUM PUMPS

Philip M. McConnell

Cryogenics Division
Institute for Basic Standards
National Bureau of Standards
Boulder, Colorado 80302

Interim Report

June 1973

FOREWORD

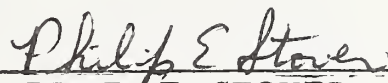This program was completed under sponsorship of the Department of the Air Force, Wright-Patterson Air Force Base, Ohio, and was funded with FY 1972 AF Aero Propulsion Laboratory Director's Funds.

This Technical Report has been reviewed and is approved for publication.

DR. C. E. OBERLY
GS-12
Physicist

FOR THE COMMANDER

DR. P. E. STOVER
GS-15
Chief, Power Distribution Branch
Aerospace Power Division

Nomenclature

A	=	area of orifice
b	=	impeller width at discharge
B	=	height of the centrifugal impeller vanes
c_m	=	meridional velocity at inlet tip
C	=	discharge coefficient
C_i	=	constants in temperature - resistance calibration correlation
D	=	centrifugal impeller diameter
D_h	=	inducer hub diameter
D_m	=	$\sqrt{D_t^2 (1\ 2\ v^2)/2}$, mean effective, inducer diameter
D_t	=	inducer tip diameter
E	=	elastic modulus
$\widehat{E}_v$	=	mechanical energy losses per unit mass per unit time
g	=	local acceleration of gravity $(9.7961\ m/s^2)$
H	=	total dynamic head
$\Delta L/L$	=	thermal strain
$\dot{m}$	=	rate of mass flow at pump discharge
n	=	pump rotative speed

NBP	$=$	normal boiling point
NPSH	$=$	$P_1/\rho_1 + V_1^2/2g - P_{v1}$, net positive
N_s	$=$	specific speed, see eq (6)
$N_{s,cav}$	$=$	suction specific speed, see eq (7)
P	$=$	absolute pressure
ΔP_p	$=$	$P_2 - P_1$, differential pressure across pump
ΔP_v	$=$	differential pressure across venturi
Q	$=$	m/ρ_2, volumetric rate of flow of pump discharge
Q_ℓ	$=$	bearing cooling flow
r_m	$=$	$1/2\ D_m$
R	$=$	resistance of thermometers
R_e	$=$	Reynolds Number of the discharge tube
T	$=$	temperature
T_λ	$=$	2. 172 K, λ-point temperature
T'	$=$	torque
u_1	$=$	tangential velocity at D_m
u_2	$=$	tangential velocity at D_2
V	$=$	average stream velocity at point of static pressure tap

w	=	relative velocity
$\widehat{W}$	=	total average 3-phase power input to motor
W	=	power per unit mass
W_f	=	effective power imparted to the fluid by the pump, defined by eq (4)
W_{sh}	=	$T'\omega$, shaft power
Z	=	vertical distance above datum plane

Greek Symbols

α	=	angle between the tangential velocity and the absolute velocity, see figure 9.
β	=	vane angle of impeller
γ	=	specific weight
η	=	efficiency
ν	=	D_h/D_t, hub ratio of inducer
ρ	=	fluid density
ϕ	=	c_{m1}/u_1, flow coefficient
φ_1	=	c_{m1}/u_1^2, inlet flow coefficient
ψ	=	$2gH/u_1^2$, head rise coefficient, at inlet
ω	=	angular velocity

Subscripts

1	=	inlet
2	=	discharge
3	=	bearing cooling passage
c	=	critical
cav	=	cavitating
h	=	hydraulic
ℓ	=	liquid
m	=	motor
n	=	normal fluid
nc	=	non-cavitating
p	=	pump
s	=	superfluid
t	=	total
u	=	ullage
v	=	vapor, volumetric
v1	=	saturated vapor at inlet

CONTENTS

LIST OF FIGURES

LIST OF FIGURES (Continued)

LIST OF TABLES

ABSTRACT

This report summarizes studies of pump charac-
teristics and performance in supercritical, normally
boiling, and superfluid helium, and also presents results
on a survey of commercially available pumps for helium
service. Experimental measurements were made on a
centrifugal pump which produced a maximum head of about
15 meters, and a maximum flow of about $2.5 \times 10^{-4} \, m^3/s$.
Performance agreed approximately with classical affinity
laws, but cavitation appeared to provide less of a perform-
ance limitation than expected. The survey turned up
several pumps which have been used in helium, though
relevant performance data is lacking.

Key words: Cavitation; helium; pump performance; pumps;
superfluid.

Liquid Helium Pumps*

Philip M. McConnell †

1. Introduction

Pumps are presently being used [1-4],[1] or considered [5], to provide forced helium cooling of superconductive magnets and power transmission lines. However, there exists little experience in pumping helium, and no pump performance characteristics with low temperature helium (2 K < T < 8 K) have previously been reported in the literature. Therefore, design and performance characteristics have been largely speculative.

A basic question which we wish to examine in this study is: What unique features are involved in the pumping of helium? The low latent heat of vaporization (about 22 J/g at 4K), low viscosity, and superfluidity are some of the unusual properties of helium (2 K < T < 8 K) which could give rise to unpredictable pump performance. On the other hand, if the helium is single phase and Newtonian, helium pumping should be similar to the pumping of single phase, low temperature hydrogen (or other cryogenic fluids); in this case the considerable work which has already been done [2, 6, 7, 8, 9, 10] could be used to advantage. Actual helium data are obviously needed to verify the feasibility and reliability of using conventional pumps to transfer the various fluid phases (e.g., LHe II, LHe I, two-phase helium, and supercritical helium),

[1] Figures in brackets indicate the literature references at the end of this paper.

to verify the pump affinity laws [11], and to check the validity of accurately predicting helium pump performance using less expensive fluids. The phase diagram for helium is shown in figure 1 (not to scale). Systems currently under study require intermittent cooling flow rates which are greater than 1.9×10^{-3} m^3/s (30 gal/min) at relatively low differential pressures. With this in mind, the study has been rather arbitrarily limited to include pumps whose design capacities are less than 6.3×10^{-3} m^3/s (100 gal/min) with relatively low total head, and to helium inlet temperatures between 2 and 8 K. The helium thermodynamic and transport properties, necessary for any pump analysis, are well known for these flow conditions [12].

The characterization of pumps for helium service is discussed in general terms in section 2., wherein we summarize the origin of some of the important pump parameters and their applications. Although many of these parameters were developed from work solely on impeller pumps, they can be meaningful when applied to other types of pumps, e.g., ejector pumps [13]. More comprehensive treatments of impeller pump design, performance, and similarity parameters are given by Wislicenus [14], Stepanoff [11], and Kovats [15], and Lazarkiewicz and Troskolanski [16]. Other pump types such as reciprocating pumps and gear pumps were also of interest, but few of these types are found for low temperature use. Also included are practical considerations involved in pumping helium--e.g., cavitation, stability of the pump, bearings, types of motor drives, etc.

The results of a survey of helium pumps are given in section 3. It includes results of an extensive review of the literature of helium pumps, and results of personal communication with various pump manufacturers whose products may be applicable for helium service.

2
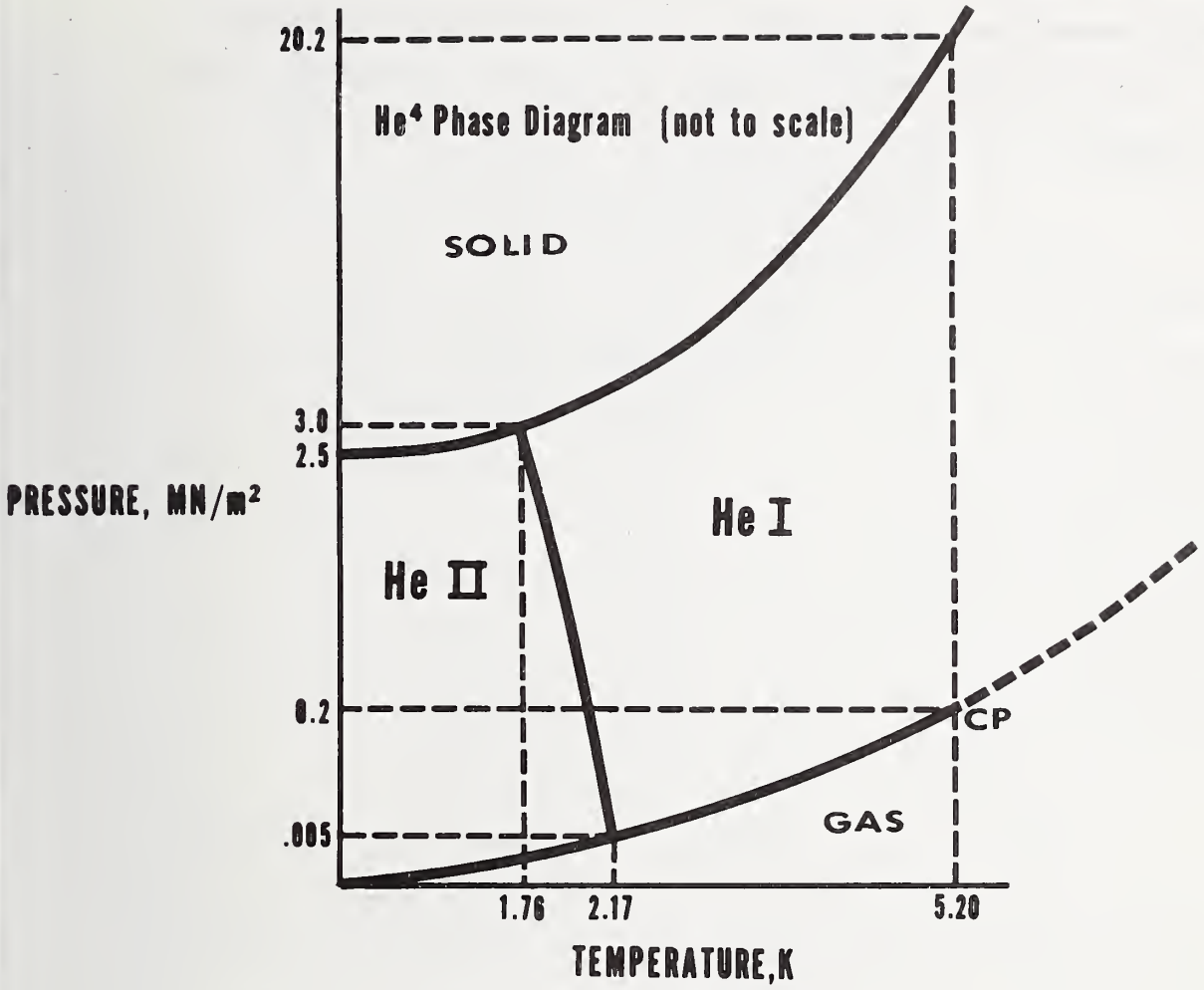
Figure 1. Phase diagram for He^4.

In section 4 we describe our own laboratory tests of a small centrifugal helium pump designed for flows up to $2.5 \times 10^{-4} \, m^3/s$ (4 gpm) with a total dynamic head of 15 meters, characteristics which may be useful for various superconductor applications where forced flow cooling may be required.

2. Pump Characterization

2.1 Mechanical Energy Balance

A typical liquid helium pumping system is shown in figure 2. The pump motor may be operated at ambient temperature, location a, or submerged in the fluid, position b. Both of the configurations have their advantages and disadvantages, which will be discussed later. The superconducting system may be located in the pump dewar or in a remotely located dewar, depending on the particular application.

The steady state mechanical energy balance [17], applied to the pump between the inlet and discharge (planes 1 and 2, respectively), can be written per unit mass per unit time as

$$\frac{\Delta V^2}{2} + g \Delta Z + \int_1^2 \frac{dP}{\rho} - \widehat{W} + \widehat{E}_v = 0 , \qquad (1)$$

where the numbers '1' and '2' denote the measured inlet and outlet stream conditions respectively, $\widehat{W}$ is the specific power input to the pump, and $\widehat{E}_v$ is the rate at which mechanical energy is irreversibly converted to thermal energy, i.e., friction losses. For an isentropic process, E_v is equal to the rate of heat removal through the pump casing between 1 and 2. Assumptions made in the derivation of (1) are that the flow is turbulent and that the gravitational acceleration, g, remains constant throughout the system. The first three terms in (1) represent the fluid or useful power per unit mass, $\widehat{W}_f$, imparted to the fluid by the pump. The pump efficiency defined as

4
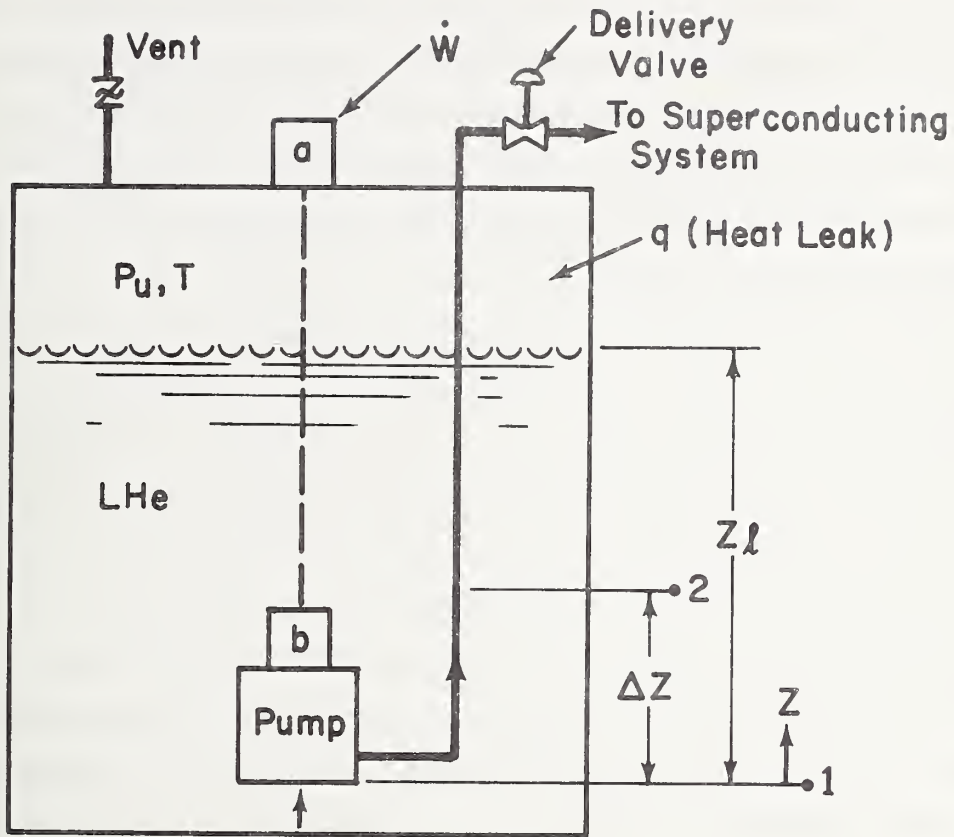
Figure 2. Schematic diagram of a liquid helium pumping system.

$$\eta = \frac{\widehat{W}_f}{\widehat{W}} = \frac{\widehat{W} - \widehat{E}_v}{\widehat{W}} \tag{2}$$

is determined from measurements of all the terms in (1) other than $\widehat{E}_v$. Since continuity of mass requires that $\dot{m}_1 = \dot{m}_2 = \dot{m}$, $\eta = W_f/W_{sh}$, where W_f is the fluid power and W_{sh} is the shaft power to the pump. It is sometimes convenient to divide (1) by g. In this case, the first three terms are referred to as the total dynamic head (H), where

$$H = \frac{\Delta V^2}{2g} + \Delta Z + \frac{1}{g} \int_1^2 \frac{dP}{\rho}. \tag{3}$$

The first two terms in eq (3) are usually much less than the third. The H has dimensions of length (usually expressed in units of the working fluid as characterized by the inlet stream conditions), and for a given pump operating at a constant speed and volume flow rate is (approximately) independent of the fluid being pumped. The fluid power can be expressed in terms of H as

$$W_f = \dot{m}g\,(H) = \gamma_1 Q_1\,(H) = \gamma_2 Q_2\,(H) \tag{4}$$

where $\dot{m}$ and Q are the rates of mass and volumetric flow, respectively, through the pump, and γ is the specific weight of the fluid.

In order to evaluate the integral in eqs (1) and (3) along a representative streamline, one must know the equation of state, $\rho = (P, T)$, how T changes with P along the streamline, and the thermodynamic path of the process from 1 to 2. For the special cases of an isothermal system, $\rho = \rho\,(P)$, and isentropic flow of an ideal gas, the integral may be easily evaluated. In the case of isothermal flow of an incompressible fluid

$$\int_1^2 \frac{dP}{\rho} = \frac{P_2 - P_1}{\rho}.$$

The assumption of incompressibility applies when the change in pressure is only a small fraction (a few percent) of the absolute fluid pressure and is usually a good assumption for most liquids and gases at low Mach numbers. Variations in density due to changes in pressure can be described by the equation

$$\Delta P = -E\,\frac{\Delta V}{V_o} = E\,\frac{\Delta \rho}{\rho_o}\,,$$

where E is a "modulus of elasticity" of the volume change ΔV [18].
The compressibility of most liquids is small, e. g. , for water
$E = 1.9 \times 10^9 \ N/m^2$ (19,000 atm) which means that a pressure increase
of $1 \times 10^5 \ N/m^2$ (1 atm) causes a relative change in density of about
0.005 percent. Liquid helium, however, is considerably more com-
pressible, e. g. , at 4.0 K, $E = 2.5 \times 10^6 \ N/m^2$ (25 atm) giving a
relative change in density of about 4 percent for $\Delta P = 10^5 \ N/m^2$ (1 atm).

In supercritical helium near the critical point, relative changes
in density of several hundred percent are possible with $\Delta P = 10^5 \ N/m^2$,
depending on the temperature. Thus, the assumption of incompressi-
bility must be carefully examined when pumping helium.

2.2 Pump Performance and Characteristics

In general, the steady state performance of a pump running at a
constant speed is described by its response to both changes in capacity,
Q (non-cavitating performance), and the net positive suction head, NPSH
(cavitating performance). The latter type of performance is only mean-
ingful in the pumping of liquids. The net positive suction head, NPSH,
sometimes referred to as the anticavitation pressure margin, is defined
as

$$NPSH = \left(\frac{P_1}{g\rho_{\ell 1}} + \frac{v_1^2}{2g} \right) - \frac{P_{v1}}{g\rho_{\ell 1}} , \tag{5}$$

where subscript 1 refers to the pump inlet and the quantity in paren-
thesis is the stagnation inlet head. As shown in figure 2, the inlet
pressure is the sum of the tank pressure (ullage pressure) and the pres-
sure due to the weight of the liquid above the inlet plane, i. e. ,

7

$$P_l = P_u + g \int \rho_\ell \, dZ \, .$$

If the liquid is in thermal equilibrium with its vapor and has a relatively low inlet velocity, then

$$P_u = P_{v1} \text{ and NPSH} = Z_\ell \, .$$

If this is not the case, accurate measurements of NPSH are much more difficult, depending on the magnitude of the slope, dP/dT, of the saturation curve [19, 20].

Non-cavitating performance:

During a typical non-cavitating pump test, the shaft speed, n, is maintained constant while the independent variable, Q, is altered by throttling the delivery valve, see figure 2. For each valve setting, the flow rate, total dynamic head, and the shaft power are simultaneously measured. The shaft power, $W_{sh} = T'\omega$ is obtained from either a torque measurement, T', or from measurements of the power consumption of the driving motor of known efficiency.

In this way, the conventional, experimental non-cavitating performance curves $H = f(Q)$, $W_{sh} = f(Q)$, and $\eta = f(Q)$ are obtained. The difficulty of accurately determining $H = f(Q)$ from theory lies in accurately calculating the losses occurring in the pump. The shape of the above curves depends strongly on the pump geometry (impeller and casing) and a similarity parameter known as the specific speed [11, 15, 16].

The specific speed,

$$N_s = n Q^{1/2}/H^{3/4} \, , \tag{6}$$

8

is usually computed[2] at the best efficiency point (b. e. p.) and is useful in characterizing types of impeller pumps; e. g., centrifugal pumps have values of N_s between about 500 and 3500.

Pumps of the same value of N_s will, regardless of differences in size and shape, tend to have similar performance characteristics. A designer uses this fact to good advantage in that testing of one pump will allow the performance of other pumps of the same N_s to be accurately predicted.

Cavitating Performance:

The cavitation performance of a pump is obtained experimentally by running a pump with a constant liquid inlet temperature at a constant capacity and speed, and observing the H, W_{sh}, and η as the NPSH is reduced. The H = f (NPSH) curve is most commonly reported in the literature [11, 21]. The above three parameters should be independent of the NPSH reductions down to a point, below which the curves typically drop rather sharply. Since the parameters are not equally sensitive to the effects of cavitation, their break-away points are usually slightly different. Motion pictures taken of pump cavitation show that some cavitation can occur in the pump without influencing the performance characteristics. At the head break-away point, however, the cavitation is sufficiently far advanced to cause partial blockage of the flow passages; this phenomenon is similar to the choking of gas flow in a convergent-divergent nozzle [15]. The shape of the H -NPSH drop-off curves for an impeller pump depends strongly on the fluid properties

---

[2] Values of N_s are dependent on the units used. In the U. S., it is customary to use N (rpm), Q (gal/min), H (ft). This dependence is also true for the suction specific speed, $N_{s, cav}$. In this survey, the U. S. units are used. To convert N_s and $N_{s, cav}$ to SI units (rpm, m^3/s, m), multiply the U. S. values by 0.0194.

and the impeller inlet geometry. A parameter which presumably describes flow similarity of geometrically similar pumps, operating in the cavitation regime, is the cavitational specific speed or suction specific speed, defined as

$$N_{s,cav} = \frac{n\,Q^{1/2}}{\left(NPSH_{cav}\right)^{3/4}} \ .$$

(7)

The suction specific speed can also be formulated as a function of several of the basic pump design parameters [22], which can include the thermodynamic effects of the fluid. High values of $N_{s,cav}$ are an indication of high speed pumps which perform well at low values of NPSH, even though some cavitation is present, e. g. , aircraft and rocket fuel pumps. Below $N_{s,cav}$ of 5,000, single-suction centrifugal pumps have poor cavitation characteristics; above values of 11,000 the reverse is true. Meaningful values of $N_{s,cav}$ result when NPSH > 0. Values of NPSH ≤ 0 are an indication of boiling or two phase flow before the liquid enters the pump.

2.3 Affinity Laws

For a family of geometrically similar impeller pumps, neglecting viscous effects,

$$Q = Q_m \left(\frac{n}{n_m}\right)\left(\frac{d}{d_m}\right)^3 \left(\frac{\eta_v}{\eta_{vm}}\right),$$

(8)

$$H = H_m \left(\frac{n}{n_m}\right)^2 \left(\frac{d}{d_m}\right)^2 \left(\frac{\eta_h}{\eta_{hm}}\right),$$

(9)

$$W_{sh} = W_{sh,m} \left(\frac{n}{n_m}\right)^3 \left(\frac{d}{d_m}\right)^5 \left(\frac{\eta_m}{\eta}\right) \ .$$

(10)

10

The subscript, m, in the above equations denotes the model or test pump and η_v, η_h, and η are the volumetric, hydraulic, and total pump efficiencies, respectively. Thus, from model pump test results, we may compute the diameter, d, and speed, n, of a prototype pump required to produce a certain Q and H. These laws can also be applied to the model (or test) pump to predict values of Q, H, and W_{sh} at speeds different than the test speeds (in this case $d/d_m = 1$).

2.4 Stability

The two major requirements of a pump are the volumetric flow discharged, Q, and the total head, between the inlet and outlet. If H is not a single valued function of Q there is a danger of surging, i. e. , the throughput hunting back and forth between two values of Q and generating dangerous or undesirable vibrations. Sudden changes in pump speed can also cause unstable pump performance. One of the advantages of polyphase A. C. motors is that the instantaneous power is constant, resulting in a nearly constant shaft power output free from torque pulsations.

The shape of the steady state H-Q curve is an indication of pump stability and depends on certain design parameters. For example, pumps which have a steep H-Q characteristic give smaller fluctuations of the discharge, Q, for considerable variations in the total head. Means of improving stability in a centrifugal pump are:

1) Reduction of the outlet angle, β_2, of the impeller vanes.
2) Reduction of the impeller outlet width, b , which increases the width ratio, d/b .
3) Reduction of the number of impeller vanes giving more slip.

11

In general, increasing the stability involves a reduction in pump efficiency and higher blade loading and hence, higher NPSH requirements. Pumps with unstable H-Q curves can sometimes be used, provided the operating point is far from the multi-valued region of the curve. For example, a typical performance curve of a vaneaxial blower [11, 23] is shown in figure 3, with the recommended operating range to the right of the unstable region. One of the disadvantages of reciprocating pumps is their tendency to produce flow pulsations [6].
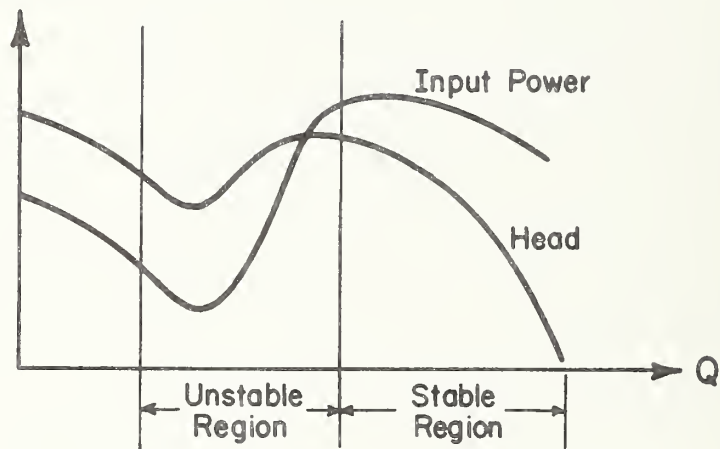
Figure 3. Typical steady state performance characteristics of a vaneaxial blower.

2.5 Helium Pump Cavitation

Tensile strengths of liquids, i.e., pressures required to produce incipient cavitation, are typically orders of magnitude lower than those predicted from theory [24]. The traditional explanation of this discrepancy between theory and experiment is that all real liquids contain submicroscopic nuclei or weak spots which relieve the applied tension. In liquid helium, the existence of many of the conventional forms of nuclei are automatically eliminated, e.g., stabilized pockets of

dissolved gas. Therefore, it was originally thought that it might be relatively difficult to induce cavitation in liquid helium. This, however, was not the case, as various researchers using different techniques found that extremely small pressure drops (of the order of 10^3 dynes/cm^2) were sufficient to cavitate helium [25]. At these incipient pressures, the observation of visible cavitation [49] coincides with audible cavitation noise in LHeI $(T > T_\lambda)$ generated from collapsing cavities, whereas in LHe II $(T < T_\lambda)$ only audible noise is detectable. The generation of visible cavitation in LHe II is made difficult by the efficient heat transfer mechanism, internal convection. As mentioned earlier, the small vapor formations which occur at incipience have an insignificant effect on pump performance. Incipient cavitation is generated at local low pressure regions along the surface of the impeller vanes, usually at the suction side of the vanes close to the leading edge. To minimize cavitation effects, the fluid should pass through the vanes with minimum disturbance, i. e., with zero angle of incidence.

As the pump speed is increased or the NPSH is reduced, cavitation continues to progress. Eventually, a point is reached where the pump passage ways become partially blocked with vapor resulting in a drop-off in the head. Pumps especially designed with an inducer stage (high suction specific speed pumps) can handle fluids which contain relatively large volume fractions of vapor without surging, damage, or head drop-off. An inducer is an axial flow impeller having a few long vanes rather than many short ones. In effect, the fluid residence time is relatively high, giving vapor formations time to recondense, leaving sufficient vane surface to impart the required head rise to the liquid before it enters the main stage impeller.

13

Cavitation data, obtained with a single pump operating in several different liquids with widely differing fluid properties, have been used to determine the relative importance of the fluid properties. One parameter which only qualitatively describes the ability of the fluid to block the flow passages in a given pump is the density ratio ρ_ℓ/ρ_v [22]. Values of this ratio, computed for several liquids, are summarized in table 1. Low values of ρ_ℓ/ρ_v indicate that blockage effects will be less severe.

Table 1. Summary of values of the saturated density ratio ρ_ℓ/ρ_v at the NBP for several fluids.

Fluid	
Water	1603
LO_2	256
LN_2	175
LH_2	53
LHe	8

Extrapolation of non-cavitating pump performance from fluid to fluid and from pump to pump is reasonably well advanced. However, predicting pump cavitation performance is still not well understood and is a matter of concern for the designer of high suction specific speed pumps. The ultimate goal is to be able to predict the cavitation performance, H = f (NPSH), solely from knowledge of the pump geometry and the fluid properties at the inlet. The predictive method developed by Ruggeri, Moore, and Gelder [21] allows the cavitation performance of a particular helium pump to be accurately determined, provided sufficient cavitation data has been taken on the same pump operating in another fluid, e.g., liquid nitrogen. Unfortunately, there are no LHe

14

cavitation data to verify the extrapolation of this predictive method to LHe. Figure 4 shows the predicted helium cavitation performance of a high suction specific speed, centrifugal pump using data obtained in liquid hydrogen [21]. The predicted helium curve shows that blockage effects occur at much lower values of NPSH than those for liquid hydrogen, i.e., at a value of the ratio of head rise coefficients of 0.9 (equivalent to a head drop-off of 10 percent) the pump in helium requires only about 6 meters of NPSH compared to 29 for hydrogen. This result is of practical importance in that for certain applications, pumps of high $N_{s, cav}$ (which tend to be expensive) may not be necessary for satisfactory operation in liquid helium.

The orientation of a submerged He-pump can influence its suction performance. For maximum NPSH the pump should be mounted vertically with the inlet near the lowest point in the dewar. When a pump is mounted horizontally a short distance below the liquid level, vapor filled vortices might be drawn into the pump when the liquid is sucked downward. This could destroy the pump performance. If the pump must be mounted horizontally, a 90 degree elbow section, with the inlet facing the dewar bottom, provides a much better inlet condition [19].

In LHe II, pump cavitation is not anticipated to be a problem because the high effective thermal conductivity of the liquid makes it difficult for cavities to grow to visible size [25].
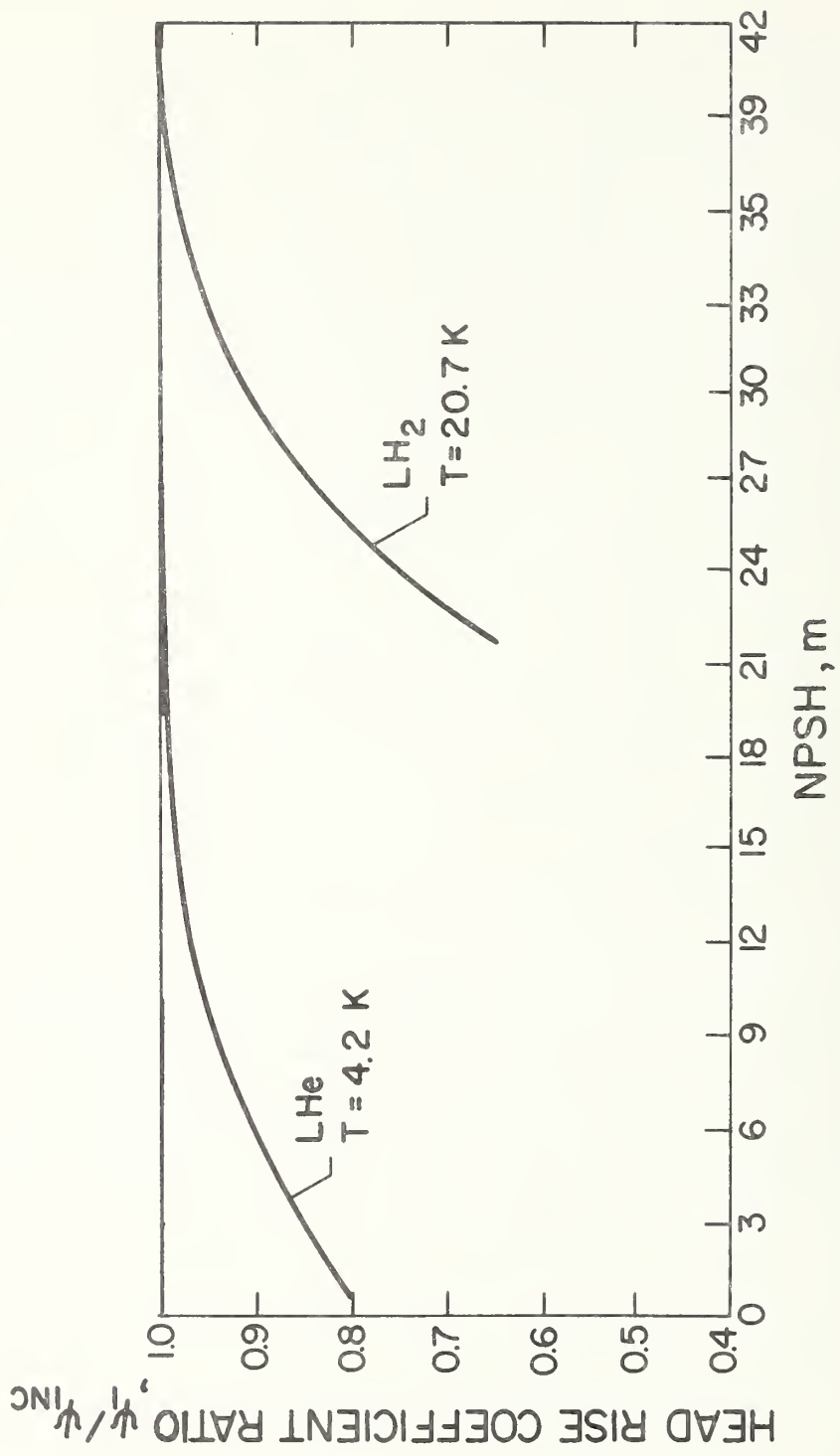
Figure 4. Predicted LHe I cavitation performance of a 67.8 mm inlet diameter, centrifugal pump; rotative speed 25,000 rpm; inlet flow coefficient, $\phi_1 = c_{m_1}/U_1 = 0.225$.

2.6 Pump Efficiency

In a helium pump, inefficiencies are not only expensive in the additional power required but also produce costly losses of fluid. This is especially true with liquid helium because of its extremely low latent heat of vaporization. The economic situation will dictate the need for gas recovery systems. An analysis by Jacobs [26] of pump losses involved in the transfer of liquid helium shows that for high discharge to inlet pressure ratios, P_2/P_1, large quantities of helium can be wasted, even though the pump may be highly efficient. The limitation of the present survey to relatively low head pumps is consistent with this analysis. Large diameter transmission lines tend to minimize P_2/P_1. If the fluid pumped is supercritical helium, the thermal effects caused by pump inefficiency can produce relatively large increases in fluid temperature and hence decreases in the density. The importance of pump efficiency in a particular system also depends on whether the pump is to operate continuously or intermittently and whether the motor is submerged or not.

When the motor is submerged (location b, figure 1) the losses are $(1-\eta_t)$, where $\eta_t = \eta \eta_m$, and η and η_m are the pump and motor efficiencies, respectively. Little information is available on the performance characteristics of cryogenic motors. Efficiencies of small induction motors are typically higher (by about 10 percent) at cryogenic temperatures than at room temperature but they decrease with motor size [8]. By using long conduction paths, the heat leak through the motor electrical leads can be made small. The main attractions of a submersible motor close-coupled to the pump are compactness, elimination of a rotating seal, elimination of heat leak down the shaft, and minimal mechanical problems due to the short shaft. These features are

favorable for flight type systems. A superconducting motor, submerged in liquid helium, might be used to drive a liquid helium circulating pump. Small, superconducting motors have successfully been operated at speeds up to 1200 rpm with all parts flooded with liquid helium [27]. However, the performance characteristics of these motors are not reported. Since superconducting motors are still in the development stage, their reliability may be poor.

For a pump operated with a room-temperature motor (location a), the only work which does not reach the pump is that dissipated by the shaft motion in the fluid and bearing friction. The amount of heat generated will depend on the surface speed and the contact area. Compared to the shaft work and the heat leak into the cryostat these friction losses are small and can usually be neglected. This configuration requires a relatively long pump shaft passing through a rotating seal to the motor. A tubular shaft made of stainless steel rather than a solid shaft greatly reduces the heat leak from the room-temperature motor to the pump. Several commercially available room-temperature, rotary seals are currently available. These seals, guaranteed to be leak tight for vacuum systems, are designed for speeds up to 10,000 rpm.

Since the density and viscosity of liquid helium is low, it can readily pass through small apertures. Because of this, a piston type pump would need close-fitting parts which in turn might produce high friction losses.

Some efficiency design criteria have evolved from the large accumulation of pump data. A few of these criteria are:

1) Pump efficiency depends on the specific speed;
   e.g., the highest centrifugal pump efficiencies
   occur in the specific speed range of 1500 to 2000.

18

2)   A wide centrifugal type impeller of small diameter
     gives higher efficiencies than a larger thinner impeller;
     the latter shape, however, gives a steeper, more stable
     H - Q curve.

3)   Pump efficiency increases with Reynolds Number, Re.
     At Re > 2 x 10^4, pump efficiencies are independent of Re.

4)   The efficiency of axial flow pumps is more nearly constant
     with variations in head rise, compared to other pump types.

5)   A vane discharge angle, β_2, of about 22-1/2 degrees should
     be used, if possible.

6)   All parts which take part in the generation of head should
     be streamlined.   All fluid passages should be smoothed
     by polishing or with special coatings.

2.7   Reliability

The reliability of a helium pump depends primarily on the bearing
life and the operation of the motor.   Hydrodynamic bearings should be
avoided because of complexity.   Since the small surface contact area
of a radial-contact ball bearing will result in a minimum of heat gen-
eration, they are recommended for impeller pumps.   At helium tempera-
tures, bearing heating is not expected to be a problem.   Modern cryo-
genic ball bearings use a glass-reinforced PTFE retainer.   The life
of these bearings with small loads over wide ranges of speed are of the
order of thousands of hours.   Submerged centrifugal pumps usually
require that one or more bearings are lubricated by the helium, which
has poor lubricating qualities.   Redmond and Bott [28] have used a
retainer impregnated with MoS_2 to provide lubrication of the balls
(440 C stainless steel) at helium temperatures.   If the ball bearings
are prevented from skidding during rapid acceleration from rest,

19

intermittent operation should not effect the bearing life. Contaminates, such as ice crystals, can be abrasive and thus a threat to long bearing life and pump reliability.

Since positive displacement type pumps (gear pumps) have relatively high weight and wear rates [8], their reliability may be poor.

Polyphase cryogenic induction motors are reliable because there are no brushes to wear out. However, D. C. brush type motors have been successfully operated in cryogenic liquids and gases [8]. At 1 to 10 watts design input, the motor reliability is lower because of low torque and interference problems due to possible contamination in the bearings. To minimize the starting torque requirements, stable pumps of low specific speed should be started with the discharge valve closed. The design and construction details of small induction motors which operate at helium temperatures are given by Redmond and Bott [28]. These motors have operated for hundreds of hours at temperatures down to 20 K and therefore are quite reliable.

3. Survey Results

3.1 Literature Review

An extensive review of the available literature has been made to assist in assessing the state of the art of helium pumping. Although no complete cryogenic helium performance characteristics are reported, supercritical helium has been pumped in several closed loop heat transfer systems and liquid helium has been pumped by a centrifugal pump and by a small reciprocating pump. Attempts to pump liquid helium below the λ-point with a mechanical pump have not been reported.

Johnston (1946 - 1947)

In his pioneering work on pumping liquid cryogens, Johnston [29, 30] tested a variety of commercially available pumps—gear pumps, diaphragm pumps, and centrifugal pumps. Although he did not do any pumping of helium, many of the problems he experienced with these commercial pumps operating in LN_2 should be applicable to the heuristic problem of using an off-the-shelf water pump in liquid helium. Of the above pump types tested, it was concluded by Johnston that a centrifugal pump, with a straight-vane impeller and carefully designed diffusion passages for outflow, worked the best.

Gottzmann (1959)

In his study of high-pressure liquid hydrogen and liquid helium pumps, Gottzmann [31] used a single stage, centrifugal forepump to provide adequate head to the liquid entering a reciprocating, high-pressure pump. This work is the first reported attempt to pump liquid helium and was apparently quite successful. The centrifugal pump was driven by a close-coupled, canned electric motor which was immersed in the liquid helium. The head rise and the NPSH required at the design conditions (presumably for water) was 24 m (80 ft) and 0. 61 m (2 ft), respectively. The forepump apparently worked trouble-free during the course of the tests. Unfortunately, neither the details of the centrifugal pump nor its helium performance data were reported.

Yonemitsu and Okada (1964)

The authors [32] describe the use of a plunger type pump to transfer liquid nitrogen to cool an infrared detector. The reciprocating plunger is driven by a room-temperature crank mechanism via a stainless steel connecting rod which passes through a warm O-ring

21

seal. The pump output is controlled by varying the speed of a room temperature motor. The piston and cylinder are made from a hard-surface material with a very fine finish in order to use the liquid as a lubricant. Details of the pump dimensions and performance characteristics are not reported.

Darrel and Schoch (1965)

A small liquid helium superconducting pump capable of transferring 6.94×10^{-6} m^3/s (0.11 gpm) with a discharge head of 0.92 m (3 ft) and 3.3×10^{-6} m^3/s (0.053 gpm) at a 1.83 m (6 ft) head is reported by Darrel and Schoch [33]. The pump is 7/8 inches in diameter and 2 inches long. A superconducting niobium piston, suspended by a thin-wall nickel bellows, is forced to oscillate at a resonant frequency of 120 Hz by 60 cycle current flowing through a superconducting coil, located below the piston. The flow rate could be adjusted by varying the amplitude of the coil current. The mass of the piston (armature) and the bellows spring constant were selected to produce resonance at this frequency. When the piston moves upward, hydrodynamic forces cause the suction valve to close and the discharge valve to open, forcing liquid through the outlet tube. These valves are disk-type made of 0.015 inch thick nylon. In reciprocating pumps, the geometry and spring design of disk-type inlet valves can affect the cavitation performance.

The reliability of this pump depends primarily on the life of the bellows, which is not well known. The leakage rate past the valves and hence the volumetric efficiency is not reported. These could be severe problems in pumps of larger size. Considerably more testing of this type of pump is needed before a true evaluation of its merits can be given.

22

Kolm, Leupold, and Hay (1965)

A small reciprocating pump using a metal bellows has been designed for circulation of supercritical helium by Kolm, et al. [34]. The pump armature is driven by a superconducting coil surrounding the outside of the pump housing. Two gravity-loaded ball valves provided unidirectional flow. Both the bellows displacement and cycling rate could be continuously controlled. A second reciprocating pump which used a double-acting stainless steel piston was also made by the authors for the circulation of supercritical helium. When operating at two strokes/sec, this second pump produced a flow rate of 6.4×10^{-6} m^3/s (0.1 gpm). The complete performance characteristics of these two pumps were not reported. The use of ball check valves in liquid have been known to cause cavitation difficulties [29].

Caine and Pradhan (1967)

The design criteria of small, submersible destratification fans (axial flow pumps) are described by Caine and Pradhan [8]. These fans are designed for liquid and gaseous hydrogen but should work approximately the same in helium. A typical fan of 48 mm (1.9 inch) tip diameter rotating at 3500 rpm produces a flow of 35 gpm and a head of about 0.67 m (2.2 ft). Typical characteristic curves and model data at the b.e.p. are given for a 0.3m (1 ft) diameter axial flow pump, with N_s = 16,000. These axial flow fans are commercially available.

Wright (1967)

The construction and performance of a double-entry centrifugal pump for transferring LN_2 are discussed [22]. Quiet and very reliable performance are reported. At the time this paper was published, the pump was commercially available. The author mentions that the pump should work in helium above the λ-point; however, no helium tests were

23

performed. The outside diameter of the pump is 48 mm. It is verti-
cally mounted and driven by a warm, 10-watt, electrical motor with
a long, stainless steel shaft. The impeller (plastic or metal) has six
unshrouded backward-curved blades. Two bearings are used: 1) to
support the impeller, and 2) to prevent whipping of the shaft. The
estimated bearing life is 10^3 hours. The fluid enters the pump from
both the top and bottom of the pump casing through 10 mm diameter
holes. The driving shaft also enters through the top hole. The use of
an unshrouded, double entry design gives low impeller bearing loads
and overcomes problems of vapor accumulation (i.e., gravity forces
allow vapor formations in the eye of the pump to escape vertically
through the top hole in the casing). Table 2 is a summary of the
reported performance obtained in LN_2.

Table 2. LN_2 pump performance reported by Wright

N	Q		Head	
(rpm)	(m^3/s)	(gpm)	(m)	(ft)
2,850	0.0	0.0	1.73	5.7
	3.3×10^{-5}	0.53	0.0	0.0
10,000	0.0	0.0	15.7	51.5
	83.5×10^{-5}	13.2	0.0	0.0

Mulder (1968)

A small electrically driven centrifugal pump (N_s = 700) was used
by Mulder [35] to circulate high pressure supercritical helium (25 atm).
A stainless steel shaft was used to minimize the heat leak from the
room-temperature motor to the pump. The centrifugal impeller, con-
sisting of 12 radial blades, was run at speeds ranging from 12,000 to
18,000 rpm. The performance characteristics of the pump are given;

24

however, these were presumably not measured in cryogenic helium.
The pump appears to be stable and has a maximum efficiency of 50
percent. At the b.e.p. the head and flow are about 77 m and
$4 \times 10^{-4} m^3/s$ (6.4 gpm). Operating problems (if any) are not discussed
by Mulder. A model of this pump is not commercially available [2].

Morpurgo (1968)

A double action piston pump was designed and used by Morpurgo
[1] to force cool a superconducting system with supercritical helium.
The pump is driven by a warm electrical motor and a long, thin rod and
crank mechanism. The pump speed is variable from 5 to 200 turns per
minute. The maximum speed corresponds to a helium flow of about
$1.17 \times 10^{-4} m^3/s$ (1.9 gpm) at a low differential pressure.

Sixsmith and Giarratano (1970)

The authors [2] describe a miniature centrifugal pump, designed
to circulate supercritical helium at high pressures (10 MN/m^2 or 100 atm).
Head-capacity data, obtained with cold nitrogen gas at several speeds,
are included. The pump is stable at all speeds tested and at 30,000 rpm
produces a maximum head rise at shut-off of about 67 m and a maximum
flow of $2.5 \times 10^{-4} m^3/s$ (4 gpm). This pump is driven by a room tem-
perature motor connected by a stainless steel shaft, about 140 mm in
length. The centrifugal impeller (25.4 mm diameter) is doubly-shrouded
and is composed of 18 backward curving vanes. In order to eliminate
surging at low flow rates, the pump was made without a diffuser. It has
several hundred operating hours with helium at temperatures from 4.2
to 30 K. However, it is not presently instrumented for the acquisition
of helium performance data. Fabrication of this pump is relatively diffi-
cult and therefore expensive.

There are two features of this pump which might give rise to poor cavitation performance in liquid helium:

1)   The inlet section (as designed) has several sharp corners which could induce premature cavitation.

2)   The high number of vanes gives relatively small flow areas. Therefore, blockage of the flow passage ways due to cavitation might be considerable.

Wagner (1970)

A small electrically driven pump and stirring unit for use at temperatures from 4 K to 350 K and pressures up to 10 MN/m^2 is described [36]. The unit was designed for circulation of gas-liquid systems for phase equilibrium experiments. A small cryogenic D. C. motor was developed especially for this work. The liquid phase is sucked by an axial flow impeller and pumped into a mixing chamber. The gas phase is driven by a six-vane, centrifugal impeller. Both impellers, connected to the same shaft, are driven by the motor. At 3000 rpm (0. 04 watt motor input) the pump produces a flow rate of 5 x 10^{-6} m^3/s (0. 08 gpm). It has been operated in nitrogen and helium for continuous periods of 80 and 4 hours, respectively. The estimated life of the ball bearings is 2500 hrs.

Heron and Cairns (1970)

A small centrifugal pump, used to circulate supercritical helium (T $\geq$ 4. 5 K) in a closed loop heat transfer experimental system, is described [3]. The pump performed trouble-free throughout the experiments. However, the authors did experience some problems with thermal oscillation in the flow loop. The complete head-capacity characteristics could not be obtained because of poor throttling characteristics

of a bypass valve. The impeller, 30 mm in diameter, has 12 straight radial vanes, 4 mm wide. The pump is driven at 18,000 rpm by a 3-phase room-temperature motor connected to a 60 mm long stainless steel shaft. The power into the pump was 24 watts. The maximum flow of supercritical helium at 4×10^5 N/m^2 (4 atm) at 6.5 K was estimated to be 7×10^{-5} m^3/s (1.1 gpm).

Mark and Pierce (1971)

The authors [37] have used axial flow fans (air blowers) to circulate liquid hydrogen through hydrogen targets. Prior to their operation in LH_2, these fans are run for a short time in LHe. The blowers are similar to those described by Caine and Pradhan [8] but are operated at speeds far below the design speed and are therefore very inefficient. These fans also have been arranged in series for higher output head. Although the fans are adequate, a small centrifugal pump better suited to the work has been developed and tested in liquid nitrogen. At the time of the report, work was in progress to build hardware to test the pump in hydrogen and helium. The pump should have the performance given in table 3.

Table 3. Estimated performance of helium centrifugal pump reported by Mark and Pierce.

N	Q		Head	
(rpm)	(m^3/s)	(gpm)	(m)	(ft)
3,400	3.3×10^{-5}	0.53	1.5	4.9
10,000	9.7×10^{-5}	1.56	13	42

Specific details of this centrifugal pump are not reported but it is believed to be similar to Sixsmith and Giarratano's [2].

Summary:

   Although much of the performance data is sketchy, the literature review shows that supercritical helium and liquid helium above the λ-point can effectively be transferred by mechanical pumps. The impeller pumps are by far the most popular and appear to offer distinct advantages of stability, wide ranges of operation, and ease of control. Such pumps are ideally suited for low head high flow situations. Reciprocating pumps on the other hand offer no obvious advantages (other than their size and shape) for producing low heads and high flows. Unfortunately, most of the pumps described are made for specific applications, are not commercially available, and are expensive to make. Since the same types of pumps are effective in LHe as well as supercritical helium, a single machine should be able to pump both phases of helium, provided cavitation effects are negligible. The cavitation effects on a pump operating in liquid helium are not presently known and pumping LHe II using a mechanical pump has apparently, here-to-fore, never been attempted. The author has recently pumped LHe II (T = 1.9 K) with a small centrifugal pump with no apparent difficulties. The results of these tests are presented in part 4 of this report.

   In future helium experiments which require the use of a pump, the installation of additional instrumentation to determine the performance characteristics would be of considerable help in the development of optimum helium pumps.

3.2 Commercially Available Pumps[3]

   As noted from the review of the literature, pumps for helium service are not readily available. In this section the results of

---

[3] The pumps referred to in this section are coded. A copy of the code list may be obtained by writing to Dr. Edward L. Brady, Associate Director for Information Programs, Institute for Basic Standards, National Bureau of Standards, Washington, D. C. 20234

personal communications with various pump manufacturers are reported. It was hoped that suitable helium pumps might only require slight modifications from the manufacturers standard line of pumps for which a complete set of water performance characteristics are usually available. The effort was concentrated on the established cryogenic pump manufacturers. However, many manufacturers of other types of pumps were also contacted. Most of the commercially available cryogenic pumps are relatively large, powerful impeller pumps and not designed for submersion or for operation at low flow rates. The helium losses for these pumps would be considerable. Many of the pump manufacturers contacted by letter did not respond while others thought that pumping helium would be impossible.

Pump A

Pumps of this basic type are made for LN_2 service. It is a single stage centrifugal pump. For helium service, the pump would be vacuum jacketed and made of stainless steel. A complete predicted performance map is available. According to the manufacturer, it produces 6.3×10^{-3} m^3/s (100 gpm) with a total dynamic head of 159 m (520 ft) and has an efficiency of 60 percent. The NPSH at these conditions is 3 m (10 ft). It is driven at 7200 rpm by a room-temperature, 2.2 kW (3 hp) motor, controlled by a variable frequency power supply. The price of the pump (including motor and power supply) is approximately $11,000.

Pump B

This submersible pump is part of an automatic LN_2 level control system. It will discharge approximately 4.9×10^{-5} m^3/s (0.78 gpm) against a head of 1.5 m (5 ft). The maximum diameter of the pump is about 50 mm. It is driven by an electric motor (10 watts) and costs approximately $400.

Pump C

This is a small, centrifugal pump designed for operation in room-temperature fluids. This model is made of 316 stainless steel and would require modifications of the bearings to operate in helium. It is driven by an electric motor at 10,000 rpm via a ceramic magnetic-coupling. Use of a magnetic coupling eliminates the need for a rotating seal. Wagner [36] found that at temperatures less than 80 K, some ceramic magnets lose much of their residual magnetism and thus their ability to transmit torque. An investigation would be needed to see if this is the case with pump C. Stray magnetic fields from the superconducting system might also affect this coupling if not shielded. A solution to these problems is to directly couple a room-temperature motor to the pump and use a rotating seal or use a close-coupled submersible motor. The total length of the motor and pump is 178 mm and the maximum width is 88 mm. The reported performance (head-capacity curve) is stable and produces about 12 m (40 ft) head at zero flow and 4.4×10^{-4} m^3/s (7 gpm) at zero head. The pump and motor sells for about $100.

Pump D

This is an all-PTFE pump which uses a nutating (360° oscillating) disk to produce pumping . The pump is sealed with a bellows and can be driven with a 37 watt (1/20 hp) motor. Although this pump is interesting and novel, materials tend to become brittle at helium temperatures which might give rise to unsatisfactory performance at these temperatures. It produces 6.7×10^{-5} m^3/s (1 gpm) with a head of about 10 meters (30 ft). Self-lubrication of the PTFE reduces friction and wear of parts. The pump has been used successfully with a wide variety of fluids; however, operation in cryogenic liquids is not reported. Because of the low viscosity of helium, leakage in this pump might be considerable. Certainly, more testing is needed before it can be accepted as a useful cryogenic pump.

Pump E

This is a small centrifugal pump designed for room temperature liquids. It produces about 8.4×10^{-5} m^3/s (1.25 gpm) at a head of 13 m (44 ft). Its appearance is quite similar to pump C and is magnetically coupled to the motor in order to eliminate a dynamic seal. Operation of this pump in helium would require modifications similar to those recommended for pump C.

Pump F

These submersible pumps are of low weight and small size and are designed for blowing air. Consequently they produce high flow at relatively low head. Driven by close coupled, submersible motors modified for cryogenic use, these pumps have been used at reduced speeds in liquid hydrogen experiments to provide forced circulation. However, at these low speeds, the efficiencies are low. They have also been run for short times in liquid helium. The head-capacity curve shows an unstable characteristic at the lower flow rates, see figure 3. These motor-pumps (modified for cryogenic use) cost a few hundred dollars, depending on the size.

Pump G

This is a submersible 100 mm (4 inch) centrifugal pump made for pumping liquid propane. Rotating at 3560 rpm, it develops a head of 43 m (140 ft) at a flow of 1.3×10^{-3} m^3/s (20 gpm). The motor should draw about 225 watts (1/3 hp) at the above output condition when operating submerged in liquid helium. However, this motor has never been operated at helium temperature. This submersible pump (including motor) costs about $2600.

31

Pump H

This is a centrifugal, cryogenic pump driven by a room-
temperature electric motor. At maximum efficiency, 44 percent,
and a speed of 1450 rpm, it will produce 5×10^{-3} m^3/s (75 gpm) with
30 m (100 ft) of head. The pump, made of 304 stainless steel, comes
with flanges at the inlet and outlet for mounting in a horizontal position,
for example, in a pipe line. The manufacturer claims that vapor binding
is prevented by having a vertical top suction. Vapor binding is inter-
preted as vapor accumulation around the impeller. The cavitation tests
of DiStefano and Caine [19] showed this configuration to be least desira-
ble in a submerged pump. The pump (without motor) is priced at about
$3000.

Pump I

This pump is a submersible, LO$_2$ pump used for NASA space
applications. The internal parts of the motor do not come in contact
with the oxygen. The motor, when corrected for the specific gravity
of liquid helium, should draw about 66 watts (0.09 hp). At the design
speed, 11,000 rpm, it produces a flow of 2×10^{-3} m^3/s (30 gpm) with
a head of 10 m (30.4 ft). Because of the many special features incor-
porated for space flight, this pump would be relatively expensive.

Pump J

This is a small stainless steel centrifugal pump designed
for operation in liquids at room-temperature (and higher). It is
driven at 3100 rpm by a canned, 50 watt (1/15 hp) motor and is
similar to pump C. Its head-capacity curve (which is stable) shows
that the pump will produce about 3.5 m of head at shut-off and at full
capacity, 1.1×10^{-3} m^3/s (16 gpm), about 1.2 meters. The water

NPSH required at full capacity is about 5 m (15 ft). The base price of the pump and motor is less than $100. Modifications similar to those mentioned earlier for pump C would be needed before this pump could be used in helium.

Pump K

Submersible axial flow pumps described by Caine and Pradhan [8] are commercially available. These are high flow - low head machines of proven reliability in various cryogenic environments.

4. Pump Tests

4.1 Description of the Tested Pump

The test pump, which was designed and fabricated in a few week's time, consists of an axial flow inducer, a centrifugal impeller, and a two-part pump housing which includes a vaneless diffuser. These parts are shown in detail in figures 5, 6, and 7, respectively. Figure 8 is an assembly drawing of these parts. The pump was designed to meet the following specifications in liquid helium at 4.2 K with a rotative speed of 628.3 rad/s (6000 rpm):

a) capacity = 2.52×10^{-4} m^3/s (4 gal/min)

b) total dynamic head = 15.2 m (50 ft)

c) efficiency > 50 percent

d) stable operation from shut-off to full flow capacity

e) cavitation free operation with NPSH $\geq$ 0.305 m (1 ft).

The inlet and discharge velocity triangles, based on the above design criteria, are shown in figure 9. The selection of β_2 = 60° was based on consideration of the desired steepness of the head-capacity curve and the required output for a given speed and impeller diameter. The choice of β_2 is important, since all the non-cavitating design constants depend on this value. To meet the stability requirement, the centrifugal impeller was made with a low number of backward curving vanes (six) and a relatively high breadth ratio, D_2/B_2. The centrifugal impeller and inducer vanes were machined with a numerically controlled mill. This allowed duplicate (or scaled) pieces to be made quickly at low cost. These rotating parts were statically balanced before final assembly. The clearances in the pump had to account for differential expansion, $\Delta L/L$, between brass and aluminum over the temperature range of 1.8 to 300 K. The magnitude of this difference is about 3×10^{-4} m/m.

The above pump parts were designed to mate to an existing 3-phase submersible, cryogenic induction motor rated at 35 watts, as shown

0.653"
(16.59 mm)

60°

FLOW

A

A

.160"
(4.06 mm)

29°

.312"R
(7.92 mm)

.080"
(2.03mm)

.050"
(1.27 mm)

Full Rad.

.016"
(.406mm)

.126"
(3.18mm)

.032"
(.813mm)

.260"
(6.6 mm)

VIEW A-A
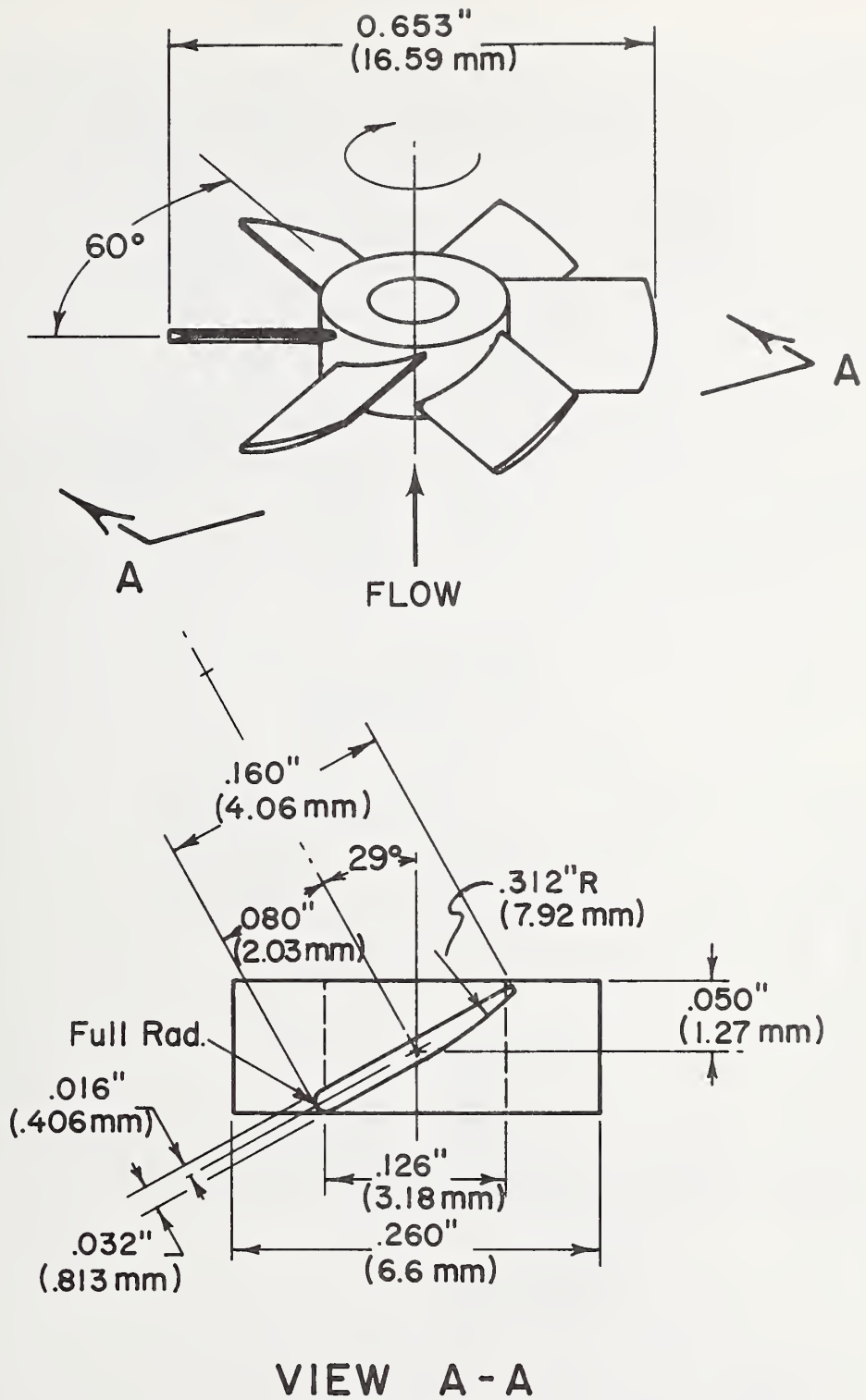
TYPICAL BRASS VANE (6 each)

Figure 5. Axial flow inducer; brass vanes are silver soldered into cuts in the hub.

35
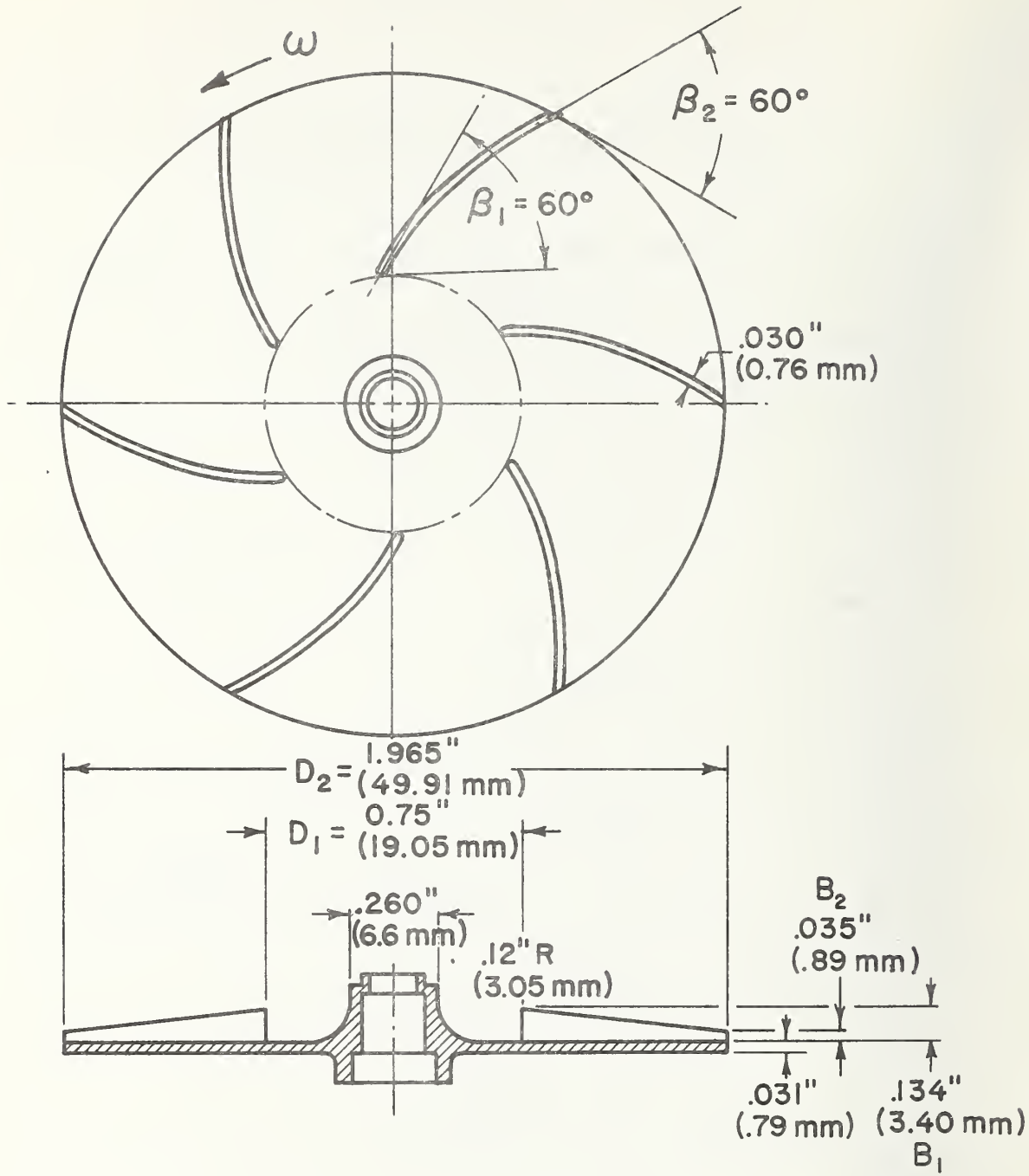
Figure 6. Centrifugal impeller for helium pump, 6061-T6 aluminum, anodized finish.
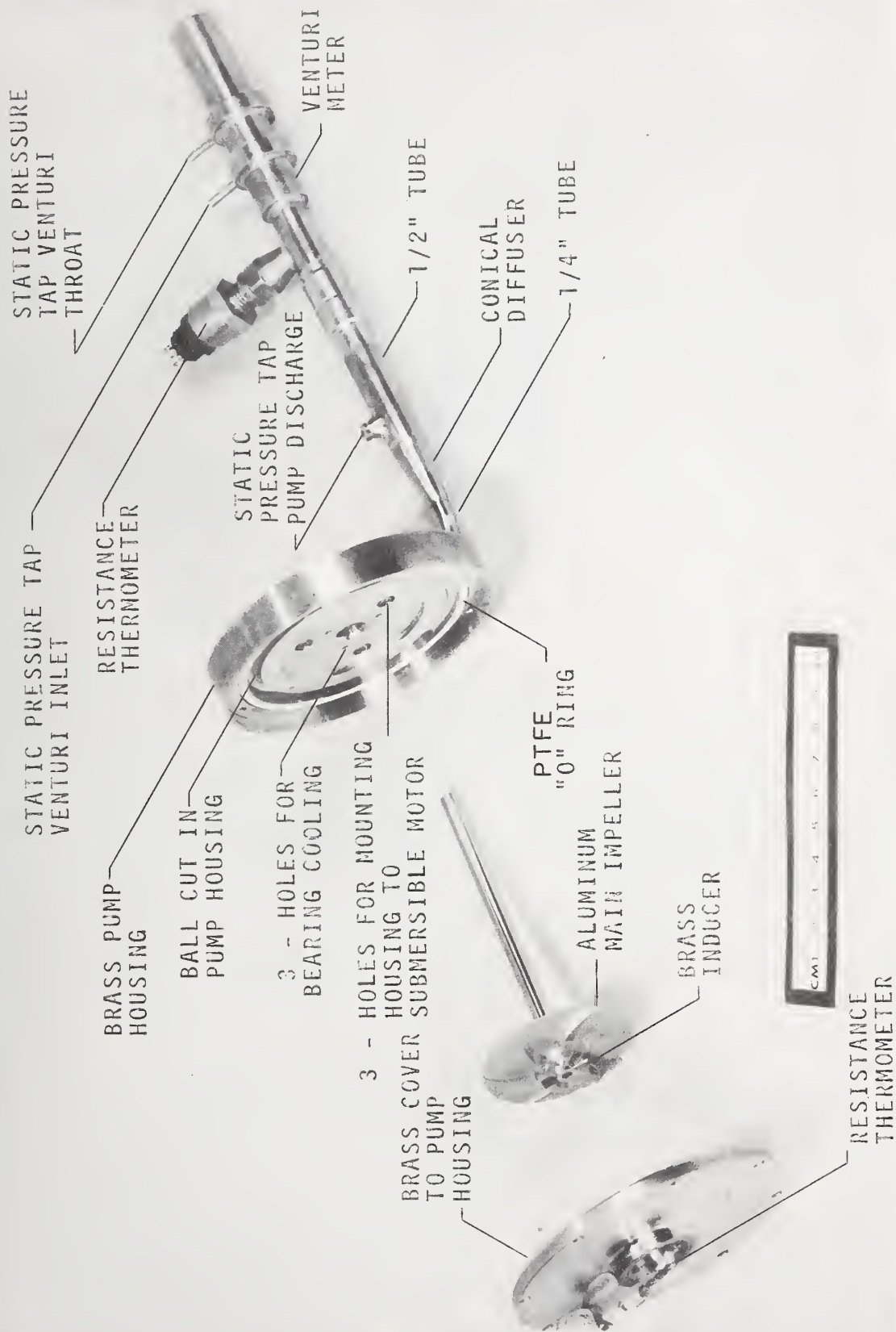
Figure 7. Photograph of helium pump parts.

STATIC PRESSURE TAP VENTURI THROAT

VENTURI METER

STATIC PRESSURE TAP VENTURI INLET

RESISTANCE THERMOMETER

STATIC PRESSURE TAP PUMP DISCHARGE

1/2" TUBE

CONICAL DIFFUSER

1/4" TUBE

BRASS PUMP HOUSING

BALL CUT IN PUMP HOUSING

3 - HOLES FOR BEARING COOLING

3 - HOLES FOR MOUNTING HOUSING TO SUBMERSIBLE MOTOR

PTFE "O" RING

BRASS COVER TO PUMP HOUSING

ALUMINUM MAIN IMPELLER

BRASS INDUCER

RESISTANCE THERMOMETER

37

Stainless Steel Tubing

Helical Compression Spring

#6-32 NC Self-locking Nut

Low-temperature Bearings with Glass impregnated, PTFE Retainer

1.6675"
(42.35 mm)

Submersible 3-Phase Induction Motor,
400 Hz, 208 VAC L-L
120 VAC L-N
Power max 35 W

.444"
(11.28 mm)

2.41"
(61.2 mm)

.950"
(24.1 mm)

Stainless
Steel
Shaft

3 Holes, .088"dia. (2.24 mm)
for Bearing Cooling

Groove for
PTFE O-Ring

.200"
(5.08 mm)

.031"
(.787 mm)

.035"
(.89 mm)

1.0"
(25.4 mm)

.10"R
(2.54 mm)

.673"
(17.1 mm)

#6-32 NC
Self-locking
Hex Nut

1.12"
(28.45 mm)

2.72"
(69.1 mm)

3.188"
(80.98 mm)

3.75"
(95.25 mm)

Figure 8.   Assembly drawing of helium pump and submersible motor.

38
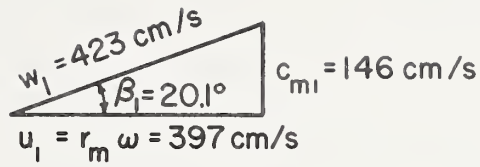
a. Inlet velocity triangle at mean effective inducer diameter, $D_m = 12.6$ mm (0.497 in); $n = 628$ rad/s (6000 rpm); $Q_t^m = Q + Q_\ell = 3.16 \times 10^{-4}$ m^3/s; zero prerotation.
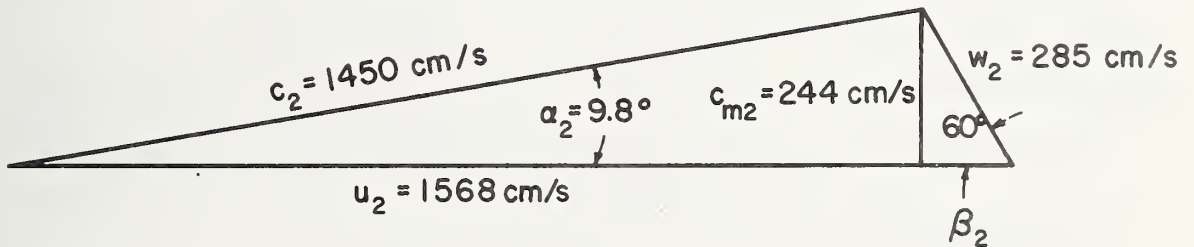
b. Velocity triangle at centrifugal impeller discharge, D_2; $n = 628$ rad/s (6000 rpm); $Q_t = Q + Q_\ell = 3.16 \times 10^{-4}$ m^3/s.

Figure 9. Inlet and discharge velocity triangles based on the design criteria.

39

in figure 8. The motor speed is controlled with a three phase, variable frequency (300 - 500 H_z), variable voltage (0 - 120 V L-N) power supply. This motor, originally made for NASA to drive miniature destratification fans [28, 8], is designed to operate over a wide range of temperatures (4 K < T < 300 K), and since it has been operated for hundreds of hours in air, gaseous oxygen, liquid nitrogen (LN_2), and liquid hydrogen (LH_2), is quite reliable. In the present studies, the motor efficiency, when running submerged in helium is not accurately known but is estimated at 35 to 50 percent [8]. Efficiencies of small cryogenic induction motors typically decrease with the size of the motor.

4.2 Test Loop and Instrumentation

The pump test loop and instrumentation are schematically shown in figure 10. The vertically mounted pump is suspended a few centimeters from the bottom of a 1.22 m deep, stainless steel, cylindrical dewar by two stainless steel support tubes. The electrical leads for the submersible motor, liquid level meter, speed sensor, and resistance thermometers are fed through these support tubes. The fluid is pumped vertically upward through a venturi flow meter, then passes through a 3/8-inch cryogenic throttling valve (flow coefficient = 1.1) and is finally discharged at low velocities through a conical diffuser. The leak rate of the throttling valve when closed and pressurized with helium gas was checked in liquid nitrogen by observing extraneous bubbles. Since at pressures twice those expected in the pump tests, only a few bubbles were occasionally emitted through the stem, the valve was considered to be sufficiently tight to determine the head rise of the pump at zero flow.

The pump speed, n, is determined from the frequency of an alternating voltage, generated from an electro-magnetic pickup, whose magnetic field is periodically perturbed by a 20-tooth ferrous gear. This gear is rigidly attached to the top of the pump shaft. The frequency is measured by a counter.
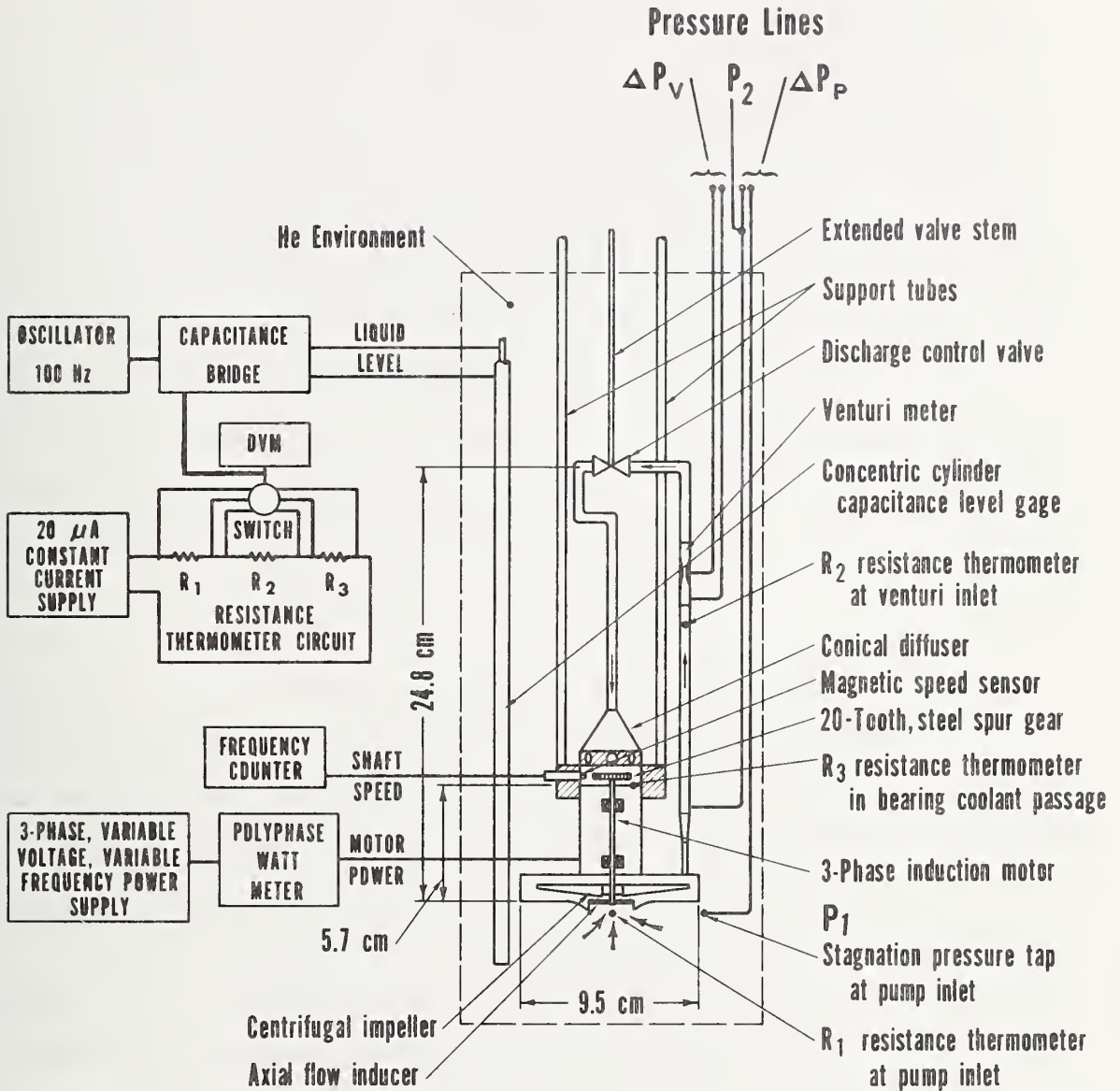
Figure 10. Schematic diagram of He-pump test loop and instrumentation.

41

The fluid discharged from the diffuser mixes the fluid surrounding the pump and helps maintain a constant bath temperature, determined by the vapor pressure above the liquid surface. Consequently, when pumping liquid helium, the height of liquid above the pump inlet is equal to the NPSH. A calibrated capacitance level gage, shown in figure 10, is used to measure the liquid level in the dewar and hence the NPSH at the pump inlet. The sensing capacitor, one leg of the capacitance bridge, consists of two concentric stainless steel tubes running the full length of the dewar. Only the very top and bottom of the outer tube are open to the bath. The bridge output voltage, measured with a DVM, was somewhat noisy, varying as much as 2.4 percent during a measurement interval of 1 minute. The precision of the liquid level measurements, as typified by the overall standard deviation of the calibration data, is 40 mm.

The fluid temperatures at the pump and venturi inlet, T_1 and T_2, respectively, are measured with calibrated, 1/8 watt carbon resistors, R_1 and R_2. The resistor R_2 is positioned halfway inside the discharge tube and tightly sealed from the helium bath. A third resistor, R_3, located inside the motor and near the top, is used to detect any significant temperature increase due to possible bearing heating; none was observed. These thermometers, powered by a constant D.C. current of 20 μA $\pm$ 0.01 μA, were calibrated in place against the saturation temperature of LHe (in equilibrium with its vapor) over the range 1.75 K < T < 5.2 K. To extend the calibration range to 20 K, the three thermometers were immersed in liquid hydrogen. The voltage drops across R_1, R_2, and R_3 were measured on the same DVM mentioned earlier. Steady background thermal emf's were subtracted out by taking two readings, one with reversed current. During the calibration, the

42

system pressure, maintained constant with a manostat to within 930 N/m^2 (7 mmHg), was measured by directly observing one of three manometers, depending on the pressure range. Systematic errors in the T-R calibration data can occur due to thermal stratification in the fluid and slight changes in resistance with time. Errors in temperature can be as high as 2 K in some liquid helium systems with severe stratification. Past experience using carbon resistor thermometers in helium indicate that they are reproducible to within 0.010 K over a period of a few months.

Over the temperature range 1.7 K < T < 20 K the calibration data fit a logarithmic expansion of the form

$$\ell n \, T = C_o + \sum_{i=i}^{6} C_i \, (\ell n \, R)^i \, ,$$

where C_o, C_1, . . . C_6 are constants. With measurements of R_1, R_2, and R_3, this function is used to compute T_1, T_2, and T_3 in the analysis of pump performance. With these curves, the total rms error of the calibration data is 0.86 percent, 0.55 percent, and 0.44 percent, respectively for T_1, T_2, and T_3.

The differential pressure across the pump, ΔP_p, and across the venturi, ΔP_v, are directly measured with differential, bellows-type, pressure gages. These measurements are used in the calculations of the total dynamic head and the rate of volumetric flow discharged, respectively. The pump discharge static pressure, P_2, and the ullage pressure, P_u, are measured with manometers. These manometer measurements are used to check the direct measurements of ΔP_p and to compute the fluid densities at the pump inlet and discharge. At system pressures equal to or greater than ambient, the manometer

measurements of P_2 and P_u are gauge pressures. With system pressures less than ambient, P_u is measured with an absolute manometer and P_2 is determined from $P_2 = P_1 + \Delta P_p$, where P_1 is the sum of pressure due to the hydrostatic fluid head above the pump inlet and P_u.

When pumping liquid helium, the unknown location of the liquid-vapor interface in the pressure lines is a source of both random and systematic error in these pressure measurements. This problem can be eliminated by using vacuum insulated pressure lines with a heater attached at a known location on the inner lines. This step, which greatly complicates the system and gives additional heat leak, was not required in the present work. In the differential pressure measurements, it is assumed that this interface occurs at the same elevation in each of the two lines since temperature differences between the different pressure lines were minimized by wrapping them with copper wire and soldering them altogether at several points.

Both differential pressure gages, sized for the pump design criteria, were calibrated over their full range against a differential manometer filled with distilled, room-temperature water. The precision of the ΔP_v gage (range 0 - 20 inches of H_2O), estimated from the standard deviation of the calibration data, is about 0.8 percent of full scale. The absolute error in ΔP_v is estimated to be less than 1.8 percent at the high flow rates and increases to about 8 percent at the lowest recorded flow rates. Similarily, the precision of the ΔP_p gage (range 0 - 100 inches of H_2O) is 0.4 percent of full scale. The absolute error in ΔP_p is estimated to be less than 4.0 percent over the range of ΔP's typically produced by the pump. The response time of both ΔP_v and ΔP_p systems (i.e. the pressure lines and gages) to sudden changes of differential pressure in the dewar is less than 5 seconds.

44

In order to accurately measure the ullage pressure, P_u, in the dewar over the entire range from 0 to 3×10^5 N/m^2, three mano-meters were used which covered the following ranges of absolute pressure:

$0 < P_u < 0.6 \times 10^5$ N/m^2,   Maximum, estimated error of pressures measured in this range is 8.3 percent.

$0.8 < P_u \leq 1.4 \times 10^5$ N/m^2,   Maximum, estimated error of pressures measured in this range is 0.5 percent.

$1.4 \times 10^5 < P_u \leq 3.0 \times 10^5$ N/m^2,   Maximum, estimated error of pressures measured in this range is 0.1 percent.

Significant thermal-acoustic pressure oscillations were not observed in any of the pressure gages during the course of these experi-ments. This is a fortuitous result, since in general, thermal oscillations and instabilities have been known to be problems of major importance in helium systems [40]. The elimination of such oscillations may partially be due to the construction of the stainless steel pressure lines, which typically consist of a length of a small diameter tube (1.4 mm i.d.), originating from the pressure source, followed by a larger tube (2.9 mm i.d.) which leaves the low temperature environment. The different sizes of line represent resonant cavities of different volumes. Therefore, the possibility of system resonance to oscillations of any one frequency are presumably reduced.

The average 3-phase power into the motor was measured with a two element, polyphase wattmeter. The power and frequency ranges of this meter are 0 - 60 watts and 25 to 800 Hz, respectively. The estimated accuracy of the power measurements is 0.75 percent.

The venturi meter used to measure the helium flow rate is shown in detail in figure 11. Since the venturi is not calibrated, its dimensions, which are based on standard forms, had to be machined accurately in order to use the recommended [41] discharge coefficient, which is a function of the tube Reynold's number, Re. When Re $> 2 \times 10^5$, the discharge coefficient is constant and equal to 0.984. It has been found experimentally that the discharge coefficient is almost the same for compressible fluids and incompressible fluids for well designed venturi meters [17]. The internal dimensions of the venturi were obtained by pouring molds of the inside contours with dental plaster, whose setting contraction is 0.05 percent. The external mold dimensions were then measured with an optical comparator. The errors in fluid density and in ΔP_v both contribute to the total error in the volumetric flow rate, estimated to be 4.1 percent at the lowest values of flow and 1.1 percent at the highest. Flow measurements in LN_2 and LH_2 have also been made in previous work, using similar venturi meters [42,43].

4.3 Results of Pump Test

During a typical (non-cavitating) performance test, the pump, started with the discharge throttling valve closed, is slowly brought up to the desired speed, n, which is maintained constant to within $\pm$ .3 percent. The measured head rise across the pump typically reaches a steady value within 20 to 30 seconds.[4] This comparatively long time appears to be associated with the creation and decay of perturbed temperature distributions in the pressure lines due to movements of cold fluid into the initially warmer lines. At this shut-off condition, $\Delta P_v = 0$, indicating zero flow through the venturi meter. There is, however, some flow through the bearing cooling passages, shown in figure 8. The magnitude of this coolant flow, Q_ℓ,

[4] Similar waiting times were also characteristic of the measured head rise when the pump was started with the discharge valve fully open.

46
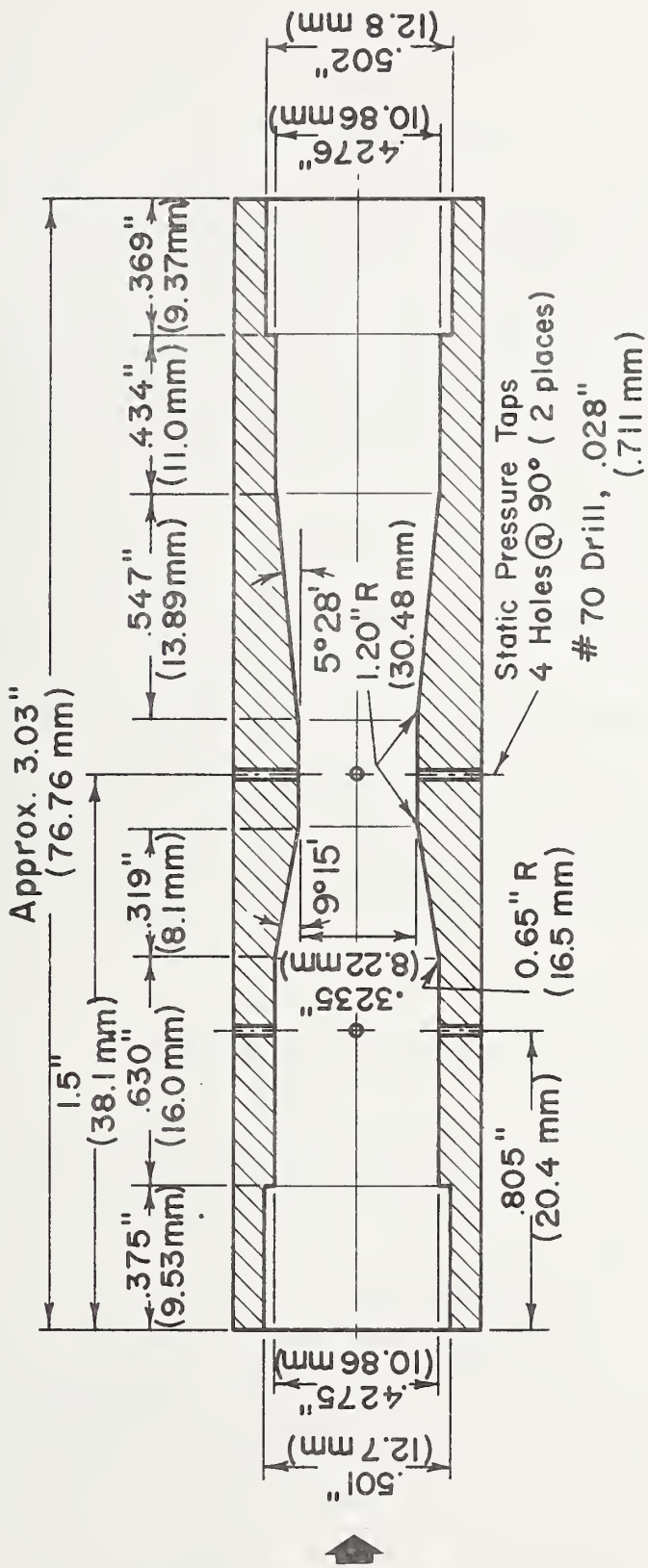
Figure 11. Venturi flow meter used in helium pump tests.

47

is not accurately known, but can be estimated from the relationship which describes orifice flow,

$$Q_{\ell} = CA\sqrt{2 \, g \, \Delta P/\rho} \; , \tag{11}$$

where C is the discharge coefficient, A is the orifice area (11.8 mm^2), and $\Delta P/\rho$ is the static head loss across the orifice. At the pump design speed, Q_{ℓ} is estimated to be about 25 percent of the design flow capacity. When the pump tests were finished, it was concluded that bearing heating was insignificant and that this forced cooling of the bearings was unnecessary.

The pump flow capacity, Q, is altered by throttling the discharge valve. For each valve setting, the static pressure rise, ΔP_p, the power consumption to the motor, W, and the helium flow rate through the venturi, are simultaneously measured. In this way, the pump characteristics, $H = f(Q)$, $W = f(Q)$, and total efficiency $= f(Q)$ are determined. Data are taken for both increasing and decreasing values of Q. The total dynamic head, generally defined for steady state conditions, is

$$H = \frac{V_2^2 - V_1^2}{2g} + (Z_2 - Z_1) + \frac{1}{g} \int_1^2 \frac{dP}{\rho} \; , \tag{12}$$

and is directly related to the power, W_f, expended by the pump on the fluid, where

$$\dot{W}_f = \dot{m} g \, (H) \; . \tag{13}$$

In the application of (13) to the present study, $\dot{m}$ is the rate of mass flow through the discharge tube, measured by the venturi meter. However,

48

the pump is also expending a certain amount of useful work in pumping
fluid through the bearing cooling passages; e. g. , at 628 rad/s (6000 rpm)
the magnitude of this rate of work is estimated to be about 0. 8 watts.
This contribution is neglected in calculations of efficiency.

If the fluid is isothermal and incompressible, the integral in
(2) is simply $(P_2 - P_1)/g\rho$. The first two terms in (2) are small com-
pared to the third. Therefore, the percent error involved in calculating
the total dynamic head is approximately the same as the error in
measuring $\frac{\Delta P}{\rho}$, which is believed to be less than 5. 3 percent. Since
typical measured temperature differences $(T_2 - T_1)$ are only a few
hundreths of a degree, the isothermal approximation is valid. However,
the incompressible assumption for pumping helium must be examined
closely. In the present tests, the values of $(P_2 - P_1)$ are at the most
$1.5 \times 10^4 \text{ N/m}^2$ (0. 15 atm), and hence, the error in the incompressible
approximation is small when pumping liquid helium. For the tests with
supercritical helium, this assumption is not valid and the integral must
be evaluated numerically.

The pump efficiency, η_p , is the fluid power divided by the shaft
power, i. e. ,

$$\eta_p = W_f / W_{sh} \text{ ,}$$

where $W_{sh} = T'\omega$. In the present tests, the motor is close-coupled to
the pump and submerged in helium. Therefore, conventional torque
measurements could not be made to determine W_{sh}. The motor efficiency
was not accurately known either. Because of these difficulties, the
total efficiency is measured and is the product of the motor efficiency
and the pump efficiency,

$$\eta_t = \eta_m \eta_p = W_f / W \text{ .}$$

49

The error in W_f is estimated to be less than 9.4 percent at low values of the mass flow rate and 5.2 percent at the high values.

Effects of cavitation on pump performance are determined by maintaining a constant liquid inlet temperature, a constant pump speed, and a given valve setting while the NPSH decreased due to helium boiloff. The total dynamic head is independent of reductions in NPSH until a critical NPSH is reached. At this point the pump passages become partially filled with vapor, resulting in a substantial drop-off in the head. Cavitation effects could also be observed by inducing two-phase flow in the pump inlet as follows: The pump is run at a constant speed, head, and flow rate at values of NPSH greater than critical with the dewar vent valve closed. The saturated liquid then self-pressurizes to a certain value. With the pump operating, the vent valve is suddenly opened. This sudden depressurization results in superheated liquid which then boils violently with appreciable entrained vapor at the pump inlet. Equilibrium and steady-state performance are restored after about 30 seconds. In this test, the pump cavitation performance was similar to the low NPSH experiments.

The pump data are summarized in table 1. The accumulated test time in liquid helium is about 8-1/3 hours and in supercritical helium about 2/3 hours.

4.3.1 LHe I, 2.3 K < T < 4.3 K

Typical performance characteristics of the pump operating in LHe I at a nominal speed of 631 rad/sec (6030 rpm) are shown in figure 12. At flow rates near the design capacity (2.52×10^{-4} m^3/s) the total dynamic head is only about 1/3 of the design head (15.2 m). The reasons for this discrepancy are not known at this time. In general, head losses can be caused by cavitation, entrance losses at the leading edges of the impeller blades, friction and hydraulic losses in the impeller

Table 4. Helium pump performance test results.

Fluid	Run	n (rpm)	W (watts)	T_1 (K)	T_2 (K)	P_1 (N/m²)	P_2 (N/m²)	ρ_1 (kg/m³)	ρ_2 (kg/m³)	H (m)	Q (m³/s)	NPSH (m)	W_f (watts)
LHeI	1.1	6000	12.80	4.17	4.16	9.36+004	1.02+005	126.05	126.57	6.96	2.31-004	0.95	2.00
	1.2	5967	12.40	4.17	4.16	1.00+005	1.06+005	126.05	126.85	6.34	2.24-004	0.95	1.77
	1.3	5961	12.30	4.23	4.23	1.01+005	1.10+005	124.43	125.31	7.20	2.19-004	0.95	1.94
	1.4	5997	10.50	4.22	4.23	1.00+005	1.10+005	124.94	125.75	9.08	1.55-004	0.83	1.73
	1.5	5991	9.90	4.20	4.21	9.42+004	1.10+005	125.41	125.45	9.42	1.33-004	0.81	1.56
	1.6	5979	9.00	4.20	4.21	9.74+004	1.10+005	125.34	125.96	10.20	4.46-005	0.76	1.19
	1.7	6000	7.00	4.18	4.20	9.60+004	1.10+005	125.75	125.99	11.11	0.00+000	0.71	0.00
	4.1	1959	1.10	4.04	3.99	8.37+004	8.49+004	128.39	129.37	0.99	0.00+000	0.84	0.00
	4.2	1945	1.20	4.04	3.99	8.34+004	8.45+004	124.36	129.24	0.90	3.81-005	0.83	0.04
	4.3	1939	1.50	4.04	4.04	8.31+004	8.41+004	124.35	129.19	0.81	2.04-004	0.81	0.05
	4.4	1951	1.59	4.04	4.00	8.28+004	8.37+004	128.34	129.16	0.71	5.12-005	0.81	0.05
	4.5	1949	1.70	4.04	4.00	8.25+004	8.33+004	124.34	129.15	0.66	5.53-005	0.40	0.06
	4.6	1942	1.70	4.04	4.00	8.22+004	8.29+004	128.34	129.10	0.63	6.61-005	0.79	0.06
	4.7	1947	1.60	4.03	4.00	8.16+004	8.27+004	126.50	129.11	0.72	7.63-005	0.79	0.06
	4.8	1950	1.41	4.03	4.00	8.16+004	8.27+004	126.49	129.04	0.90	6.61-005	0.79	0.06
	4.9	1953	1.10	4.03	3.99	8.12+004	8.27+004	126.50	129.17	1.19	0.00+000	0.79	0.00
	4.10	1959	1.60	4.02	3.94	7.99+004	8.04+004	126.67	129.23	0.45	8.31-005	0.14	0.05
	5.1	6027	9.20	4.17	4.16	9.42+004	1.09+005	125.99	126.96	11.79	0.00+000	0.74	0.00
	5.2	6021	10.00	4.04	4.18	9.61+004	1.08+005	124.53	126.28	9.77	1.20-004	0.73	1.46
	5.3	6024	11.70	4.17	4.18	9.49+004	1.04+005	125.95	126.05	4.70	2.04-004	0.71	1.69
	5.4	6006	12.00	4.03	4.18	9.49+004	1.02+005	125.86	126.16	5.44	2.22-004	0.66	1.60
	5.5	6016	12.20	4.17	4.17	9.46+004	1.01+005	125.99	126.16	5.26	2.33-004	0.64	1.51
	5.6	6003	11.90	4.03	4.01	9.38+004	1.00+005	126.00	126.14	5.37	2.25-004	0.60	1.49
	5.7	6003	11.50	4.16	4.17	9.32+004	1.00+005	126.11	126.32	6.10	2.11-004	0.57	1.59
	5.8	5997	10.70	4.17	4.17	9.28+004	1.02+005	126.07	126.33	7.33	1.77-004	0.53	1.60
	5.9	6027	10.10	4.17	4.17	9.28+004	1.03+005	124.45	126.48	8.49	1.43-004	0.49	1.57
	5.10	6009	6.65	4.03	4.19	9.25+004	1.06+005	126.07	126.14	10.88	1.32-004	0.43	0.00
	5.11	6021	13.70	4.02	4.07	7.98+004	9.59+004	124.60	128.71	5.15	2.31-004	0.14	1.50
	5.12	6207	3.60	4.03	4.00	7.99+004	8.09+004	128.55	129.00	0.85	1.01-004	0.09	0.11
	6.1	3744	2.86	4.04	4.02	8.38+004	8.89+004	124.40	128.90	4.06	0.00+000	0.35	0.00
	6.2	3749	3.20	4.03	4.01	8.37+004	8.87+004	128.45	129.06	3.96	3.82-005	0.35	0.19
	6.3	3757	3.90	4.03	4.01	8.34+004	8.75+004	128.45	129.10	3.40	2.04-004	0.35	0.37
	6.4	3741	4.42	4.03	4.01	8.28+004	8.62+004	128.47	129.01	2.75	1.15-004	0.32	0.40
	6.5	3756	4.81	4.03	4.01	8.26+004	8.53+004	128.44	128.92	2.30	1.48-004	0.30	0.43
	6.6	3744	4.60	4.03	4.01	8.23+004	8.47+004	128.44	128.88	2.05	1.71-004	0.31	0.44
	6.7	3747	4.40	4.03	4.01	8.16+004	8.47+004	124.45	128.92	2.34	1.66-004	0.26	0.49
	6.8	3750	4.10	4.03	4.01	8.16+004	8.50+004	124.45	128.92	2.62	1.57-004	0.25	0.52
	6.9	3760	3.80	4.03	4.01	8.12+004	8.51+004	124.45	128.93	3.09	1.43-004	0.25	0.56
	6.10	3766	3.20	4.03	4.01	8.04+004	8.54+004	128.50	128.94	3.46	1.32-004	0.23	0.58
	6.11	3757	4.01	4.03	4.01	8.04+004	8.54+004	128.55	128.94	4.01	1.01-004	0.22	0.51
	6.12	3750	6.70	4.03	4.03	8.03+004	8.77+004	128.41	128.50	2.02	1.56-004	0.10	0.40
	7.1	5562	6.20	3.31	3.30	3.74+004	5.06+004	138.08	138.76	9.43	0.00+000	0.77	0.00
	7.2	5553	9.70	3.41	3.41	4.20+004	5.15+004	137.59	137.59	7.17	1.44-004	0.71	1.43
	7.3	5553	10.80	3.29	3.28	3.41+004	4.45+004	139.37	134.74	5.37	1.80-004	0.67	1.32
	7.4	5553	11.30	3.23	3.22	3.41+004	4.45+004	139.04	139.39	4.70	1.98-004	0.65	1.27
	7.5	5553	11.60	3.23	3.22	3.40+004	3.94+004	139.04	139.32	4.46	2.13-004	0.60	1.30
	7.6	5550	4.90	3.22	3.21	3.41+004	4.05+004	139.07	139.27	4.90	2.01-004	0.59	1.34
	7.7	5550	3.22	3.22	3.21	3.36+004	4.23+004	139.07	139.46	6.53	1.51-004	0.56	1.36
	7.8	5550	2.10	3.19	3.14	3.24+004	4.33+004	139.39	139.40	6.16	8.98-005	0.56	1.00
	7.9	5544	7.00	3.14	3.15	3.02+004	4.24+004	139.90	140.17	8.90	3.66-005	0.52	0.45

51

Table 4. Helium pump performance test results. (Continued)

| Fluid	Run	n (rpm)	W (watts)	T_1 (K)	T_2 (K)	P_1 (N/m²)	P_2 (N/m²)	ρ_1 (kg/m³)	ρ_2 (kg/m³)	H (m)	Q (m³/s)	NPSH (m)	W_f (watts)
LHE1	8.5	5997	13.00	2.29	2.38	3.82+003	1.11+004	145.82	145.43	5.39	2.41-004	0.34	1.85
	8.6	5997	11.50	2.29	2.38	4.49+003	1.49+004	145.82	145.51	7.44	1.90-004	0.34	2.02
	9.1	6000	7.40	3.10	3.06	2.31+004	3.93+004	140.22	140.92	11.77	0.00+000	0.30	0.00
	9.2	6004	11.10	3.32	3.31	2.58+004	3.74+004	138.08	138.15	8.69	1.52-004	0.28	1.79
	9.3	6004	12.60	3.25	3.24	3.53+004	4.42+004	138.85	139.18	6.77	1.98-004	0.25	1.83
	9.4	6007	13.70	3.22	3.21	3.24+004	3.93+004	139.13	139.32	5.31	2.23-004	0.19	1.62
	9.5	6003	13.70	3.18	3.18	3.18+004	3.87+004	139.50	139.68	5.30	2.23-004	0.17	1.62
	9.6	5995	12.30	3.16	3.16	3.03+004	3.99+004	139.73	139.98	7.19	1.80-004	0.12	1.77
	9.7	6015	10.70	3.13	3.14	2.99+004	4.25+004	139.98	140.28	9.26	1.27-004	0.09	1.61
	9.8	6018	7.50	3.07	3.09	2.80+004	4.28+004	140.50	140.78	10.76	3.65-005	0.09	0.54
	12.1	7156	17.60	4.11	4.12	9.01+004	9.90+004	127.11	127.15	7.52	2.72-004	0.37	2.55
	12.2	7155	17.10	4.12	4.13	8.98+004	9.95+004	126.97	127.04	8.20	2.61-004	0.29	2.66
	12.3	7149	16.00	4.10	4.20	8.91+004	1.01+005	127.24	125.57	9.89	2.29-004	0.26	2.78
	12.4	7149	14.75	4.09	4.10	8.66+004	1.01+005	127.53	127.99	11.37	1.92-004	0.23	2.73
	12.5	7152	13.50	4.08	4.09	8.58+004	1.02+005	127.68	128.15	12.76	1.48-004	0.20	2.38
	12.6	7152	11.70	4.07	4.09	8.45+004	1.02+005	127.87	128.30	14.35	9.38-005	0.14	1.69
	12.7	7155	11.25	4.07	4.09	8.43+004	1.03+005	127.87	128.31	14.73	7.65-005	0.12	1.42
	12.8	7152	9.40	4.05	4.06	9.32+004	1.03+005	128.09	128.82	15.48	3.82-005	0.10	0.75
	12.9	7161	17.60	4.05	4.06	8.28+004	9.13+004	128.09	128.30	7.12	2.5-004	0.07	2.27
	12.10	7161	17.60	4.05	4.06	8.33+004	8.95+004	128.09	127.92	5.21	2.10-004	0.06	1.37
LHFII	8.1	3225	2.40	1.91	1.95	3.87+003	7.74+003	145.50	145.58	2.71	2.54-005	0.38	0.10
	8.2	3228	2.90	1.91	1.95	4.14+003	7.88+003	145.50	145.58	2.63	3.59-005	0.38	0.13
	8.3	3225	3.50	1.94	1.98	2.65+003	5.65+003	145.55	145.63	2.11	5.06-005	0.37	0.15
	8.4	3234	4.20	1.95	2.01	2.50+003	4.50+003	145.57	145.68	1.47	1.11-004	0.35	0.23
	14.1	3243	4.40	1.85	1.90	2.16+003	4.47+003	145.43	145.49	1.74	1.46-004	0.20	0.36
	14.2	3240	4.50	1.88	1.93	2.41+003	4.66+003	145.47	145.54	1.68	1.39-004	0.20	0.33
	14.3	3225	2.40	1.87	1.92	2.45+003	7.45+003	145.45	145.52	3.50	2.54-005	0.18	0.13
	14.4	3240	2.60	1.86	1.90	2.35+003	6.85+003	145.44	145.49	3.16	4.69-005	0.16	0.21
	14.5	3237	3.10	1.86	1.91	2.41+003	6.65+003	145.44	145.49	2.98	5.08-005	0.15	0.22
	14.6	3231	3.50	1.86	1.91	2.46+003	6.20+003	145.46	145.51	2.64	6.23-005	0.13	0.23
	14.7	3231	4.00	1.87	1.92	2.30+003	5.42+003	145.46	145.53	2.23	8.80-005	0.12	0.28
	14.8	3243	4.34	1.49	1.94	2.29+003	4.79+003	145.48	145.55	1.82	1.1-004	0.11	0.30
	14.9	3231	4.40	1.90	1.95	2.55+003	4.46+003	145.49	145.57	1.71	1.27-004	0.10	0.31
SC HE	10.1	6010	11.90	4.40	4.82	2.72+005	2.78+005	121.03	121.07	5.67	2.30-004		1.55
	10.2	6010	11.30	5.15	5.15	2.74+005	2.80+005	107.36	108.08	5.77	2.40-004		1.46
	10.3	6006	9.80	5.30	5.30	2.41+005	2.88+005	98.62	100.53	7.67	2.12-004		1.60
	10.4	6018	8.80	5.37	5.39	2.81+005	2.89+005	91.43	93.30	9.60	1.68-004		1.47
	10.5	6018	7.00	5.45	5.46	2.81+005	2.91+005	80.72	86.53	12.05	1.09-004		1.12
	10.6	6012	6.00	5.48	5.50	2.74+005	2.84+005	69.94	78.14	14.07	6.94-005		0.75
	10.7	5997	5.20	5.51	5.52	2.74+005	2.85+005	60.98	69.97	15.93	3.66-005		0.40
	10.8	5998	4.80	5.51	5.51	2.72+005	2.42+005	57.56	68.70	16.55	0.00+000		0.00

52
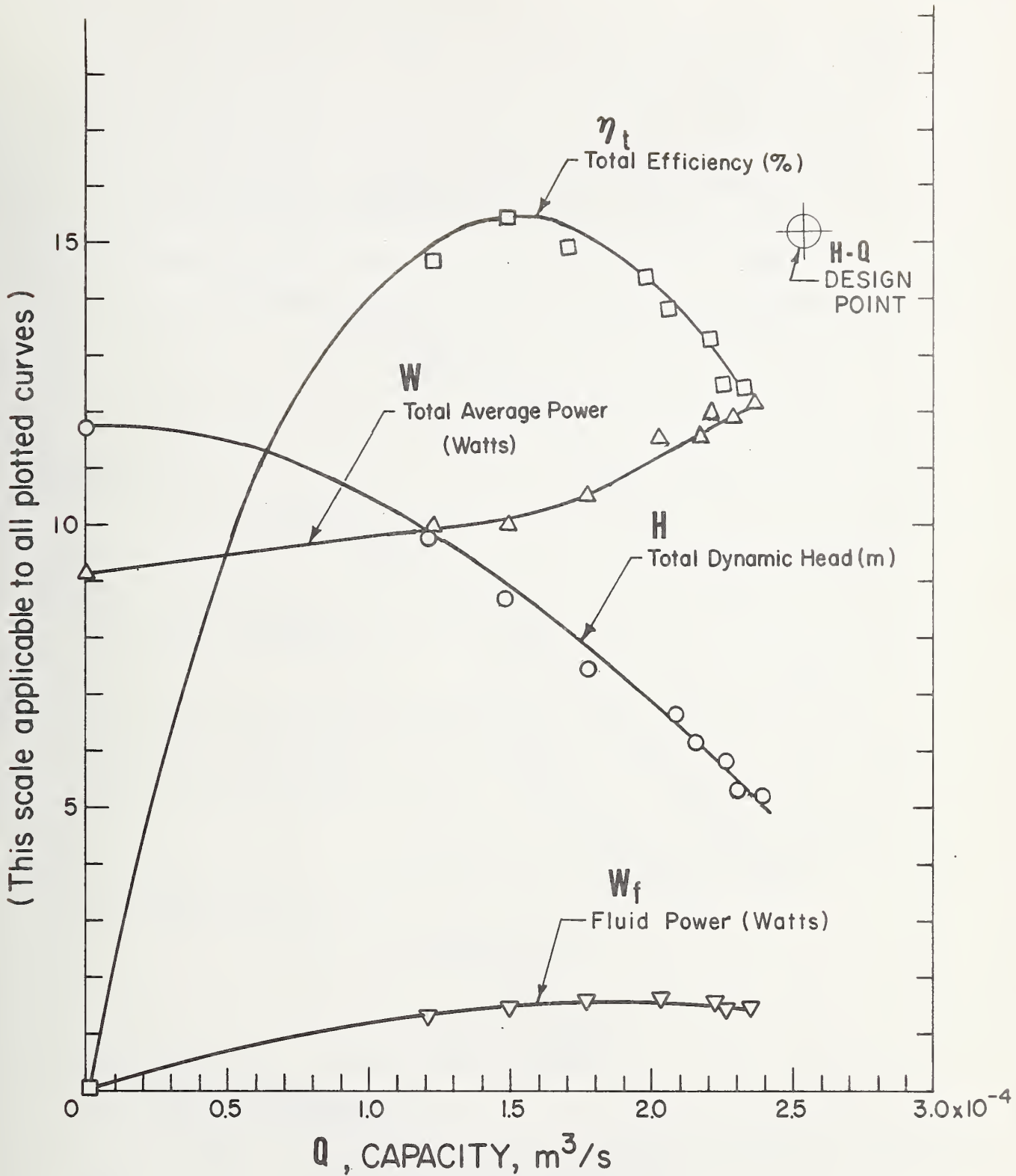
Figure 12. Typical performance characteristics of He-pump operating in LHeI; T = 4.15 K; n = 631 rad/s (630 rpm); 0.19m ≤ NPSH ≤ 0.7 m.

passages, and losses in the diffuser. The latter three factors are associated with the hydraulic efficiency, η_h. In these tests, cavitation is ruled out as a possible explanation because the developed head was independent of the NPSH when NPSH > NPSH$_C$. At the design point, the specific speed, $N_s = n \text{ (rpm)} \sqrt{Q(m^3/s)}/TDH(m)^{3/4}$, is 12.3, (638 [ft, gpm]). For small, single stage centrifugal impellers, the hydraulic losses, $1 - \eta_h$, increase rapidly at low specific speeds and might be as high as 0.35 for the test pump [12].

The maximum total efficiency, about 16 percent, occurs at a flow of about $1.5 \times 10^{-4} m^3/s$. The specific speed at this point is 14.8 (765 [ft, gpm]). Using the typical values of the motor efficiency [8] (about 35 percent at 10 watts) the maximum pump efficiency, η_p is estimated to be about 46 percent. The $H = f(Q)$ characteristic is seen to be a monotonically decreasing function which is an indication of good stability. The shape of this curve is similar to that typically found with low specific speed pumps [39].

The pump was tested in LHe I at several different speeds and with different bath temperatures. The data points produce smooth TDH = f (Q) as shown in figure 13. Constant speed data taken at different temperatures is shown in curve 5.

The affinity laws for a given pump are:

$$Q = Q_1 \left(\frac{n}{n_1}\right) \left(\frac{\eta_v}{\eta_{v1}}\right),$$

$$H = H_1 \left(\frac{n}{n_1}\right)^2 \left(\frac{\eta_h}{\eta_{h_1}}\right),$$

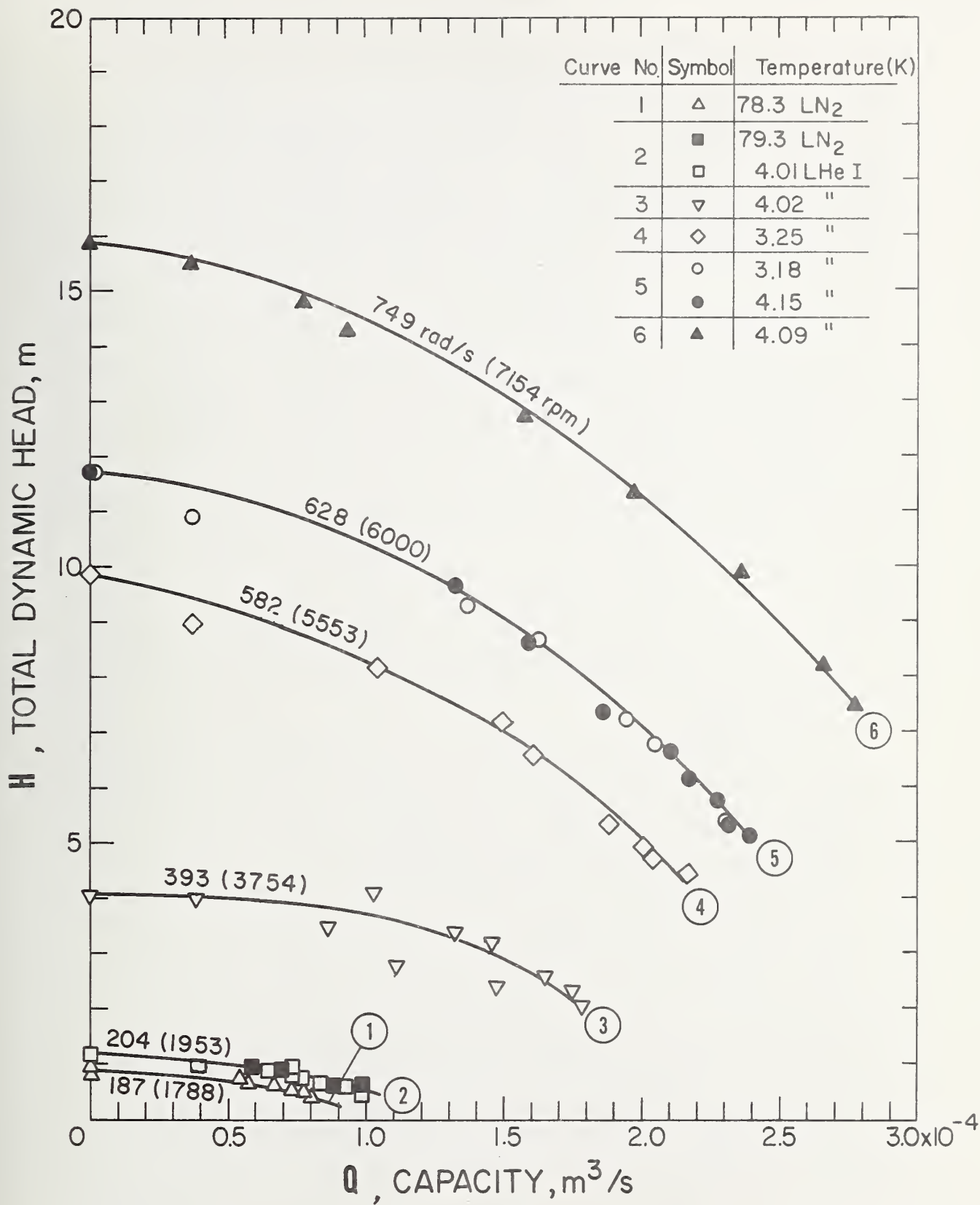$$W_{sh} = W_{sh,1} \left(\frac{n}{n_1}\right)^3 \left(\frac{\eta_{p1}}{\eta_p}\right). \tag{4}$$

54

Figure 13. Total dynamic head-capacity performance curves in
LHeI; 3. 18 K ≤ T ≤ 4. 15 K.

55

The subscript "1" in the above equations denotes known test conditions and η_v, η_h, and η_p are the volumetric, hydraulic, and total pump efficiencies, respectively. These laws can be applied to a test pump to predict values of Q, H, and W_{sh}, at speeds different than the test speeds. It is generally assumed that the efficiency ratios are equal to unity, in which case the head-capacity curves are parallel [44], e.g., in figure 13, curve 3 is predicted from curve 2. However, curves 4, 5, and 6 are slightly steeper than the low speed curves, 2 and 3; i.e., values of H, and Q predicted for the high speeds from the low speed data, are typically higher than the actual data points. Such effects have been reported by others [2] and indicate that the volumetric and hydraulic efficiencies are slightly less at the higher speeds. From (4), the higher rotative speeds give higher heads at the impeller tip and hence, higher leakage losses and rates of bearing coolant flow. Such "losses" tend to shift head-capacity curves to the left [1]. Hence, plugging of the bearing cooling holes would probably give data which are in closer agreement with the affinity laws.

Liquid nitrogen data are given in curves (1) and (2) of figure 13. The nitrogen runs were restricted to lower speeds because of the motor power limit. At the same speed, curve 2, the nitrogen data are not significantly different from the LHe I data. This result is important from a practical standpoint, since the cost of liquid helium is much higher than LN_2. In these tests, the pump Reynolds number at the inlet, about one order of magnitude higher with LHe than with LN_2, has no apparent effect on the performance. Typical values for LHe I and LN_2 are 4×10^5 and 5×10^4, respectively. Reynolds number effects in centrifugal pumps are usually secondary and are negligible above 2×10^4 [45].

The effects of cavitation on the H-Q performance were investi-
gated at two different speeds, the design speed, 628 rad/s, and the
maximum speed produced by the power supply, 749 rad/s. The helium
bath temperature was nominally 4.1 K. The data shown in figure 14,
were taken with the throttling valve fully open. The limiting or critical
NPSH ($NPSH_c$) is only about 0.09 m ± 0.04 m (3.5 in ± 1.6 in). At
values of NPSH >$NPSH_c$, the head is essentially independent of the
NPSH. However, when NPSH < $NPSH_c$, cavitation causes the head to
drop off rapidly. In this regime, the rotative speed of the induction
motor tends to increase by several percent and the pressure drop
across the venturi meter decreases, presumably because of reductions
in fluid density. Since the percent error in the NPSH measurements
is relatively high at these low values, the shapes of the cavitation curves
are not precisely known. The limiting NPSH is significantly lower than
expected. This is an important result. It suggests that a pump of
simple design can be used to pump liquid helium with relatively little
liquid cover. The tendency of cavitation to block the impeller flow
passages is probably less severe with LHe I compared to other liquids
because of the exceptionally low density ratio, $\rho_\ell / \rho_v \approx 8$ at the normal
boiling point [22]. Because this ratio is temperature sensitive, the
limiting helium NPSH is also expected to be temperature dependent.
Variations in the pump $NPSH_c$ with inlet temperature have previously
been reported by Ruggeri and Moore [21] for liquid hydrogen. The
above explanation is only qualitative and is certainly not the whole story.
Additional helium cavitation data are needed to give insight into the
general problem of accurately predicting cavitating pump performance.
By replacing the existing inlet nut, shown in figure 8, with one which
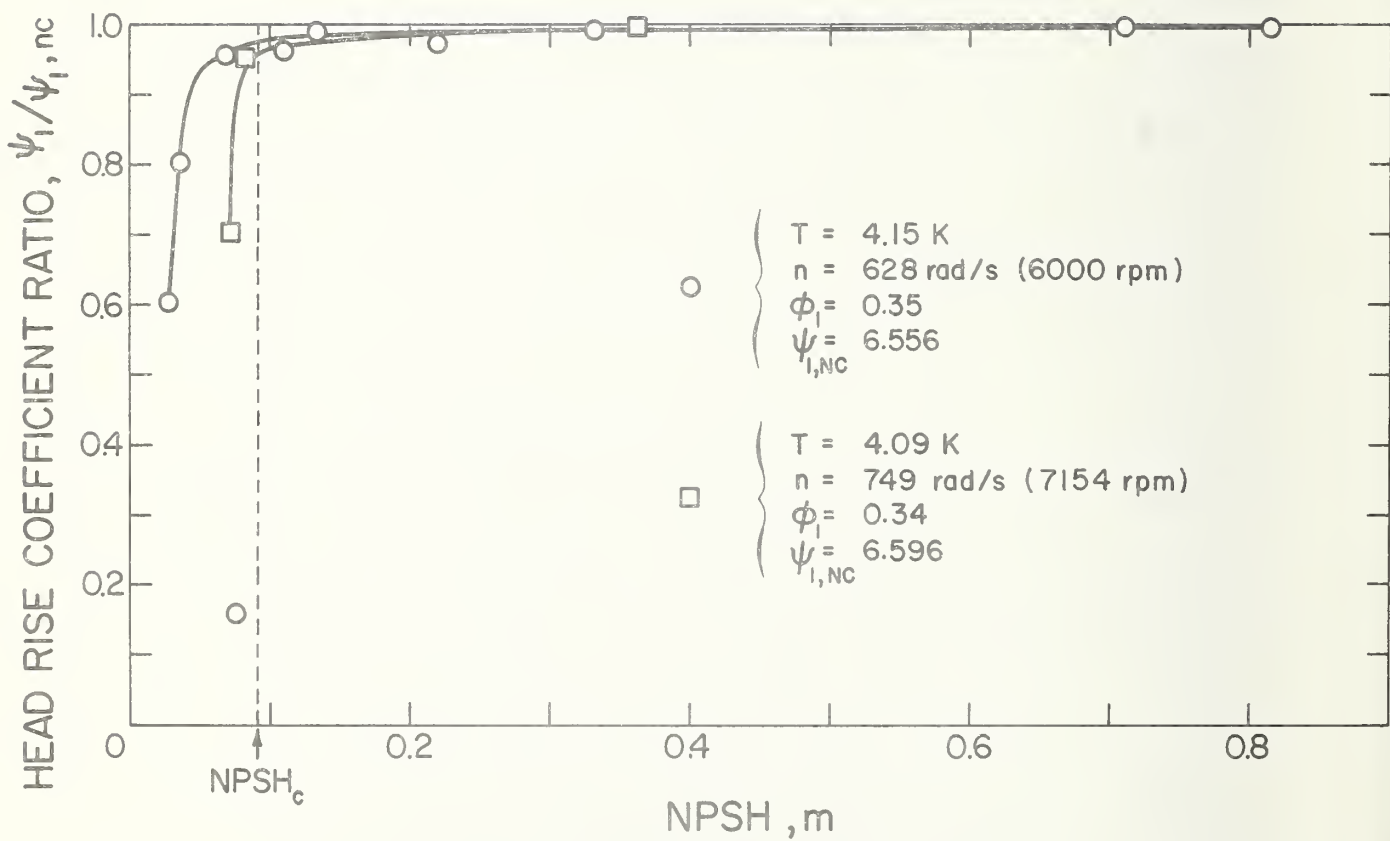is hydrodynamically smooth, even better cavitation performance might
be possible.

Figure 14. Pump cavitation performance in LHeI.

4. 3. 2 Supercritical Helium, 4. 7 K < T < 5. 6 K

The pump was given one test run near the design speed in super-critical helium. During this test, 2.69×10^5 N/m^2 $\leq P_1 \geq 2.77 \times 10^5$ N/m^2 and 4. 80 K $\leq T_1 \leq 5.51$ K. Without the stabilizing influence of bath liquid-vapor equilibrium, the pump temperature was difficult to control and tended to increase with time. In the derivation of the total dynamic head, eq (2), a steady-state process is assumed. In this test with supercritical helium, the process is really one of unsteady-state. However, since the time involved in the acquisition of each data point is short, the use of the total dynamic head is still considered meaningful. The integral $\int_1^2 dP/\rho$ is evaluated numerically for each data point using the equation of state [12] for supercritical helium and assuming an isothermal process. The resulting performance curves are shown in figure 15, with the values of the average pump temperature and density shown next to the H- Q data points. The final values of fluid density near shut-off are about 1/2 the starting density near full capacity. That the highest temperatures and lowest densities occurred near shut-off is a result of the test procedure and not a property of the pump.

Superposition of the H-Q curve in figure 15 over that obtained with LHe I at near the same speed, figure 9, shows that values of H obtained in supercritical helium are considerably higher than those of LHe I at comparable values of flow capacity, which should not be the case [15]. This discrepancy might have been caused by some systematic error in the pump differential pressure measurements and in the temperature measurements obtained from R_2. A thermodynamic analysis [46] of the pump conditions (5. 5 K, 2.5×10^5 N/m^2, and 50 percent efficiency) shows that values of dT/dP can be about 1 K/10^5 N/m^2. Then with a dP $\approx 10^4$ N/m^2 (. 1 atm), which was typically observed, dT ≈ 0.1 K.
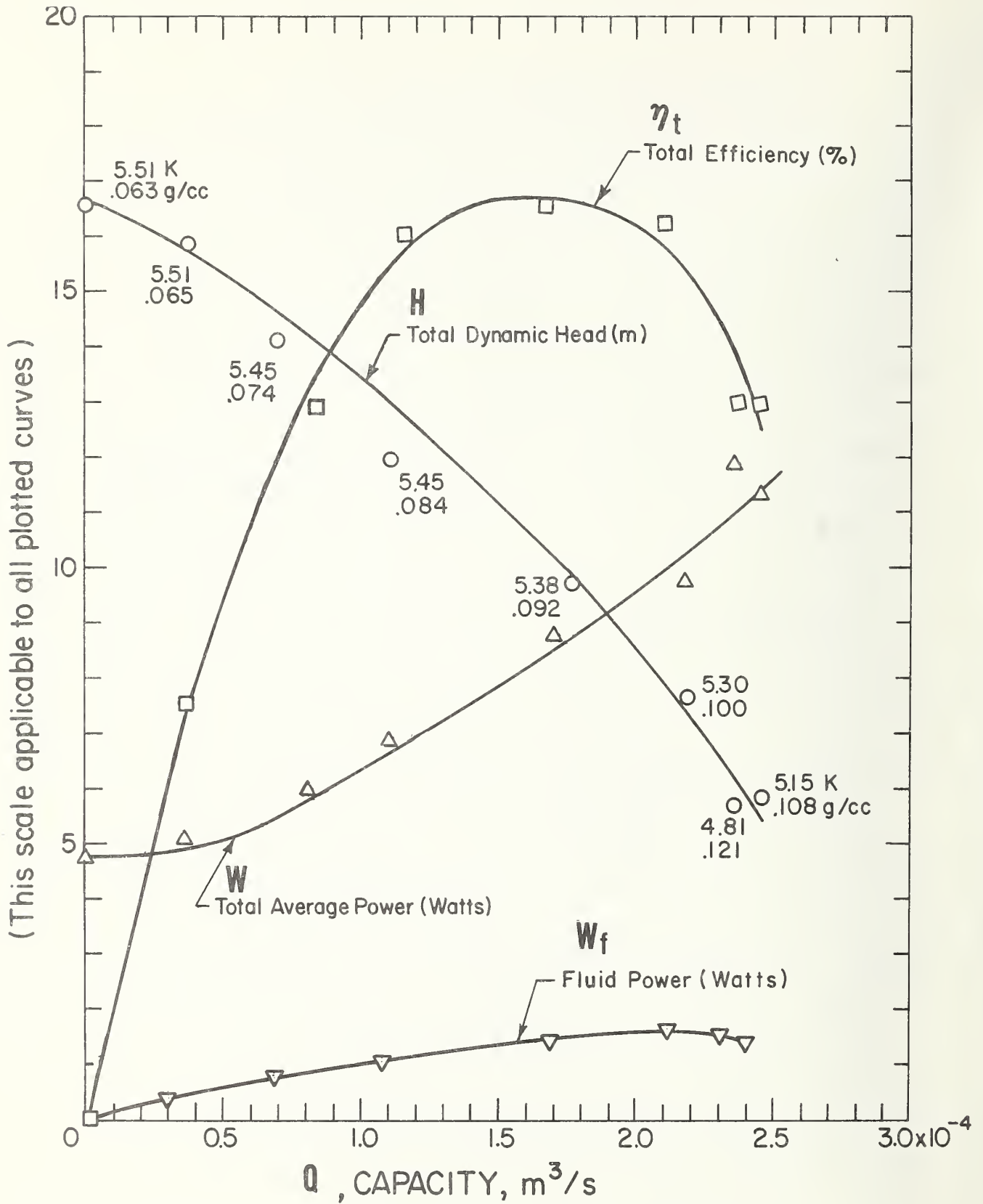
Figure 15. Pump performance in supercritical helium, n = 630 rad/s (6011 rpm).

60

This is about one order of magnitude higher than that obtained with a similar analysis for the liquid state. Such variations in temperature could give errors in fluid density of approximately 20 percent in this near-critical range, which could possibly account for some of the discrepancy. The measured temperature difference $(T_2 - T_1)$ however is only a few hundreths of a degree, but since R_2 is located some 100 mm from the impeller outlet and the thin wall discharge tube is not insulated, some heat transfer between the bath and the discharge tube occurred. Any heat transfer between the two should tend to reduce the temperature of the discharge stream at station 2.

4.3.3 LHe II, $1.8\,K < T < T_\lambda$

At saturated vapor pressures, a transition from LHe I to LHe II occurs when the temperature $T_\lambda = 2.172$ K. At this temperature, called the λ-point, visible bubble formations which normally occur during vacuum pumping of the bath suddenly cease, a result of the liquid's anomalously high thermal conductivity; the transition from LHe I to LHe II can therefore be easily recognized. At $T > T_\lambda$, LHe I behaves as an ordinary Newtonian fluid, and is referred to as "normal helium." In contrast to this, however, the macroscopic properties of LHe II at $T < T_\lambda$ cannot be described by the classical laws of fluid mechanics. Its behavior is most simply described phenomenally by a two-fluid model. The two fluids, termed the "normal fluid" and the "superfluid," have temperature dependent densities such that

$$\rho_n + \rho_s = \rho,$$

where ρ is the ordinary (observed) density of liquid helium. Since the liquid at $T < T_\lambda$ is an assembly of He^4 atoms which are all identical, the two-fluid model does not imply that LHe II is a mixture of two real

fluids. This model, which correlates a wide variety of experimental results, postulates that the superfluid component carries zero entropy and experiences no flow resistance. Comprehensive treatments of the two-fluid model, experiments done in LHe II and their interpretation are given, for example, by Donnelly [47] and by Wilks [48].

Attempts to use a mechanical pump to transfer LHe II have not been reported in the literature. The present experiments in LHe II are therefore believed to be the first attempts to pump superfluid helium. Although they were not designed or intended to investigate the basic physics of pumping superfluid, the two experiments in LHe II showed that LHe II (with approximately 50 percent mass fraction superfluid) can easily be pumped without significantly increasing the temperature of the fluid.

In one experiment, the pump was run at a constant speed and throttling valve setting while the bath temperature was reduced from above to below the λ-point. The results of this experiment are shown in figure 16. The total dynamic heads and the volumetric rates of flow measured in LHe II are not significantly different than those in LHe I. With these data, the main impeller tip speed and relative velocity at D_2 are of the order of 10 m/s. Therefore, the superfluid component is envisaged to be highly turbulent. At the lowest temperature, $T \approx 1.9$ K, approximately 50 percent of the liquid mass is superfluid. In these data, the measured temperature rise across the pump, $(T_2 - T_1)$, is of the order of a few hundreths of a degree.

In another experiment the apparent constant speed performance characteristics were measured. The term "apparent" is used because in LHe II measurements of the rate of volumetric flow using a venturi meter are ambiguous [38]; i.e., the flow of the superfluid component through the venturi may not contribute to the measured pressure drop. The same argument can be applied to the differential pressure measured across the pump. The resulting pump performance data taken at a
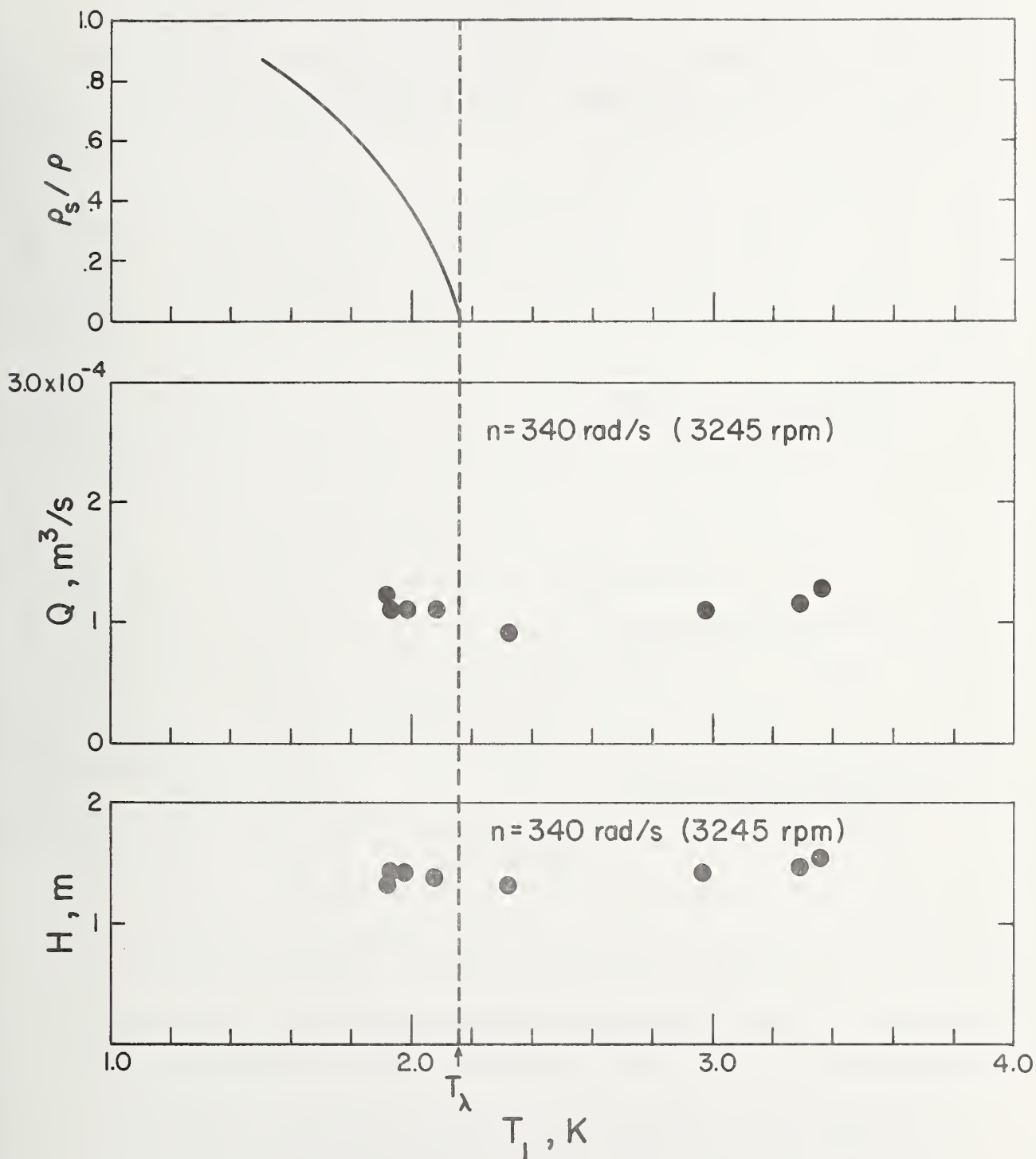
Figure 16. Pump performance in LHeI and LHeII; n = 340 rad/s (3245 rpm).

63

nominal temperature of 1.89 K, are given in figure 17. The curve drawn through these H-Q data is obtained from the low speed pump data obtained with LHe I (curve 2, fig 13) and use of the affinity laws. The solid circles represent data taken several days previous to those represented by the open ones. The curves of total efficiency and total average power as a function of Q (fig. 17) are dissimilar compared to those typically obtained in LHe I (fig. 12) and supercritical helium (fig. 15). As mentioned earlier, it would be more meaningful to plot the shaft power and the pump efficiency rather than the total quantities. Measurements of the shaft power to the pump should be incorporated in future work.

It should be noted that the overall performance in superfluid helium was not greatly different from that which would be scaled by classical hydrodynamics from measurements in normal helium--the difference being certainly less than a factor of two. Probably this comes about because the impeller tip velocity far exceeds the "critical" velocity of helium (a few centimeters per second) at which vorticity is generated in the superfluid. The tangled mass of vortices, so generated, have been shown to move approximately in accordance with classical hydrodynamical equations in many experiments. Our results are in qualitative accord with this fact.

During the experiments with LHe II, the time for both differential pressure gages to reach steady values was measurably increased. The significance of this observation is not well understood at the present time and may partially be caused by film flow inside the pressure lines. However, the slower response times did bring to mind critical velocity experiments which show that the superfluid component will (sometimes) not interact with a solid surface moving relative to the fluid because of its frictionless like behavior. In future pump experiments in LHe II, it would be interesting to see if critical velocity effects exist.
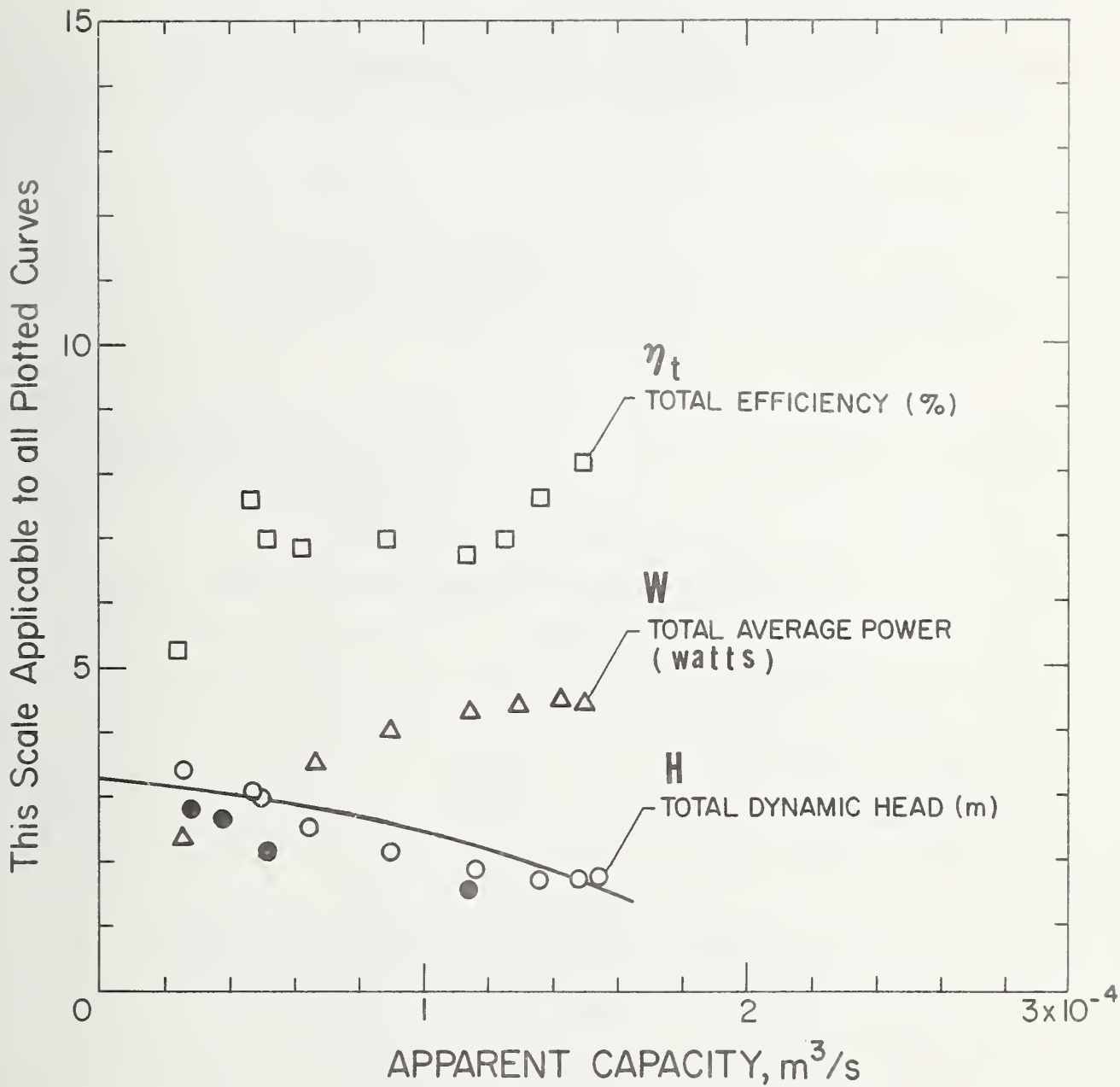
64

Figure 17. Performance characteristics of He-Pump operating in LHeII; T = 1.89 K; n = 339 rad/s (3237 rpm); 0.105 m ≤ NPSH ≤ 0.204 m.

65

4.3.4 Comparison of the H-Q Data

Using the pump affinity laws, all of the H-Q data were normalized to the design speed, 628 rad/s. The results, summarized in figure 18, show that the LHe I data fall in two zones depending on the speed. The two zones appear to be off-set by a pure translation in Q about the same order of magnitude as the estimated "leakage" through the bearing cooling holes, $Q_\ell \approx 0.6 \times 10^{-4}$ m^3/s. At the lower flow rates, the supercritical data are considerably higher than all the other data. The LHe II data are dispersed, with several points falling below the two zones. Possible reasons for these latter deviations have been discussed earlier.

4.3.5 Reliability

The reliability of the helium pump depends on the life of the low temperature ball bearings and the operation of the submersible motor. The induction motor used in these tests has good low temperature starting characteristics and is highly reliable because there are no brushes to wear out. The helium environment provides adequate bearing cooling but gives little lubrication to the balls. The ball bearings used in these experiments, made of 440 C stainless steel, are retained with glass-reinforced PTFE, impregnated with M_oS_2. The M_oS_2 provides the lubrication. Under normal operating conditions the maximum bearing life is estimated to be of the order of 10^5 hours. Since skidding of the balls is prevented during rapid motor acceleration by a spring preload (see fig. 8), the bearing life should not depend on the duty cycle. Impurities such as ice crystals can be highly abrasive and therefore are a threat to long bearing life and pump reliability. For this reason, special care was taken to eliminate traces of water from getting into the helium bath.

The start-up reliability of the pump was studied in LHe I at T = 4.1 K by periodically starting and stopping the pump, while subjected to a certain load. The nominal load condition, n = 628 rad/s (6000 rpm),

66

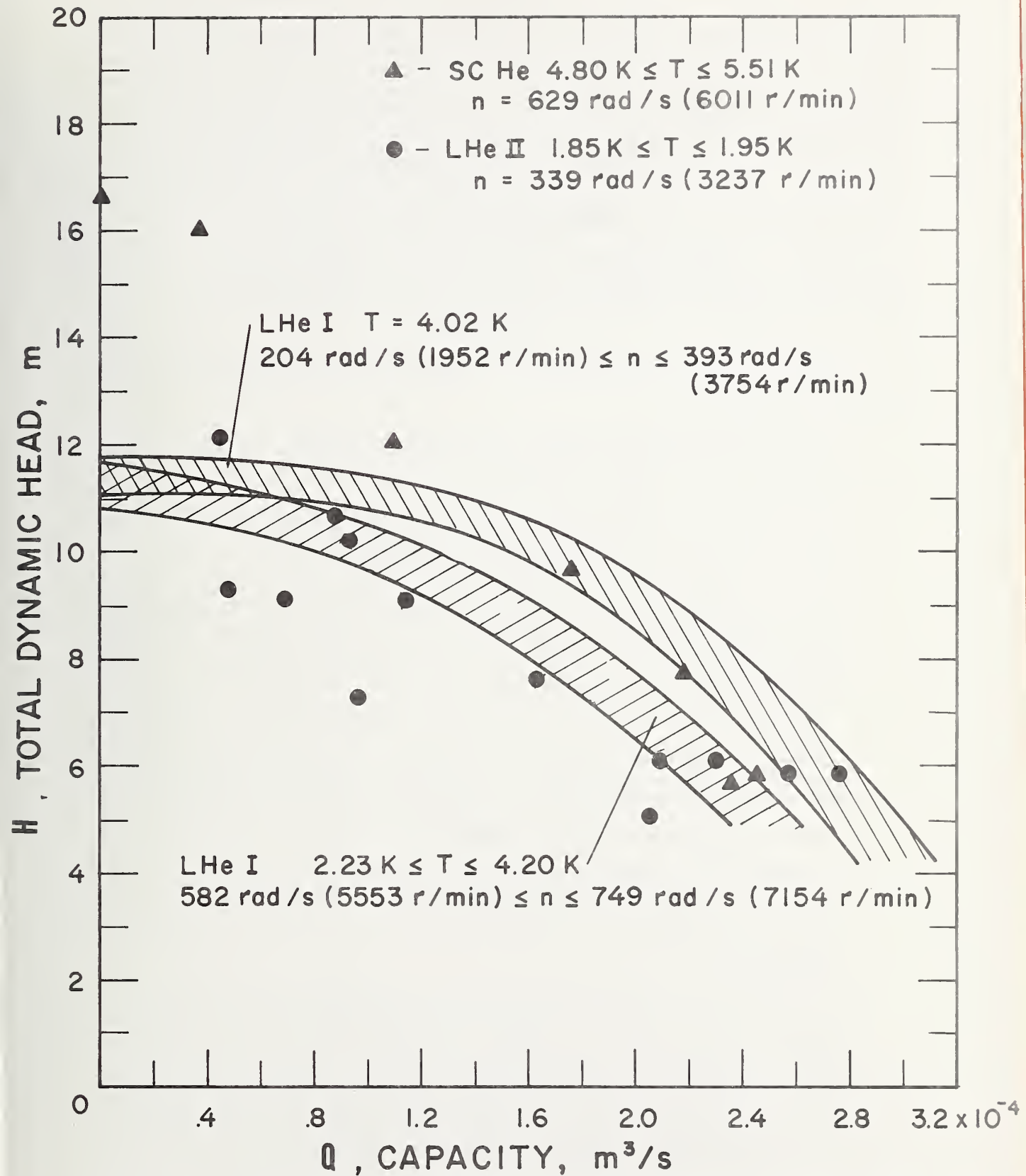Figure 18. H-Q data normalized to the design speed, 628 rad/s (6000 rpm).

head rise ≈ 5 m, and Q $\approx 2.5 \times 10^{-4}$ m/s, was chosen arbitrarily. Typical time response curves of the head and capacity are shown in figure 19. The pump is allowed to run at steady conditions for about 60 seconds. Fifty (50) such test cycles were performed with no anomalous behavior observed. For all 50 values of the steady state data, the maximum variation in head was 4.0 percent and the maximum variation in capacity was 5.5 percent. Approximately 30 additional switchings were also performed during the course of running the standard performance tests.

5. Conclusions

The following is a summary of conclusions formulated from the results of this work.

1. A pre-induced, single-stage impeller pump is a simple, controllable, and reliable method of generating forced helium flow.

2. A single-stage inducer-impeller pump of simple design can be used to pump all phases of helium from 1.85 K to 5.5 K.

3. A simple inducer-impeller pump can operate satisfactorily in LHe I and LHe II with little liquid cover. This result may not be universal and needs further testing and evaluation.

4. Results of non-cavitating pump performance in liquid nitrogen can be used to estimate non-cavitating pump performance in LHe I.

5. The pump affinity laws are applicable to the non-cavitating helium pump performance curves provided leakage effects are accounted for. Additional work is required to improve the design of helium pumps so that the design point is closer to the measured performance.

6. The non-cavitating performance of geometrically similar pumps of different size might be estimated using the results of the present tests and the pump scaling laws [16, 15, 11]. Since the validity of the scaling laws applied to helium pumps has yet to be tested, the accuracy of such predictions would be unknown.
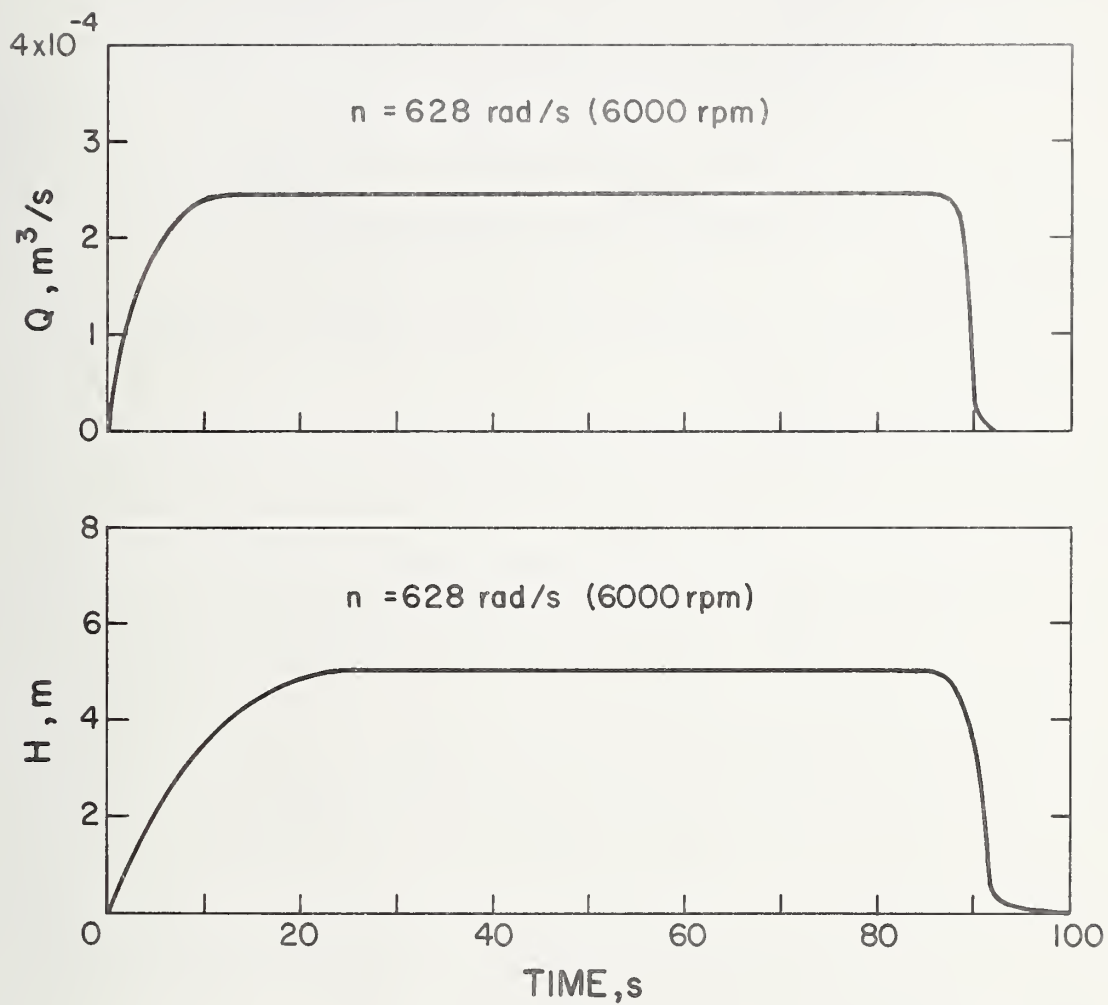
68

Figure 19. Typical reliability test cycle.

7.   The helium performance of different pumps whose specific speed at the best efficiency point is approximately 15 (780 [ft, gpm]), might also be estimated using the results of the present tests, see for instance Stepanoff [11], p. 176. Such predictions are subject to the same uncertainties as noted in 6.

6.   Recommendations for Future Work

Further insight into the detailed behavior of the pump and the relative importance of some of the parts would have been determined from the following:

1)   Determine the pump efficiency from torque measurements or from motor efficiency.

2)   Obtain additional pump cavitation data in liquid helium and in liquid nitrogen or hydrogen to evaluate the performance prediction method developed by Ruggeri, Moore, and Gelder [21,39].

3)   Eliminate the bearing cooling flow of the present design. We know now that this is not necessary and it adds uncertainty to the flow measurements.

4)   Compare performance with and without the inducer.

5)   Streamline the entrance hub nut for better cavitation performance.

6)   Increase the discharge vane angle of the centrifugal impeller to give a higher head at the design flow.

7)   Add pressure taps in the pump housing to determine

   1)   leakage flow past the inducer,
   2)   the head rise across the inducer and the centrifugal impeller,
   3)   the diffuser efficiency.

Such instrumentation would give insight for improving the present design.

Of the above recommendations, items 1 and 2 are considered to be the most crucial.

70

Systematic errors which may have occurred due to thermal gradients in the pressure lines could possibly be eliminated in future work by using pressure transducers designed to work at helium temperatures. This would also be a necessary step for automating the data acquisition and would help remove the ambiguity from pressure measurements made in LHe II.

7. References

1. Morpurgo, M., A superconducting solenoid cooled by forced circulation of supercritical helium, CERN Report 69-25, Geneva (1969).

2. Sixsmith, H., and Giarratano, P., A miniature centrifugal pump, Rev. Sci. Inst. $\underline{41}$, No. 11, 1570-1573 (1970).

3. Heron, K., and Cairns, D. N. H., Experiments on a pumped supercritical helium test loop, Central Electricity Research Laboratories Report RD/LIN 190/70 (1970).

4. Keilin, V. E., and Klimenko, E. Yu, Cryogenic problems of forced cooled superconducting systems, Cryogenics $\underline{12}$, No. 4, 292-296 (1972).

5. Snowden, D. P., Superconductors for power transmission, Sci. Am. $\underline{226}$, No. 4, 84-91 (1972).

6. Scott, R. B., Cryogenic Engineering, pp. 263-267 (Van Nostrand, New York, N. Y., 1959).

7. Daney, D. E., Ludtke, P. R., Chelton, D. B., and Sindt, C. F., Slush hydrogen pumping characteristics, Nat. Bur. Stand. (U. S.), Tech. Note 364 (1968).

8. Caine, G. H., and Pradhan, A. V., Pumps or fans for destratification of hydrogen liquid and gas, Book, Adv. in Cryogenic Eng. $\underline{13}$, Ed. K. D. Timmerhaus, pp. 728-738 (Plenum Press, New York, N. Y., 1968).

9. Urasek, D. C., Meng, P. R., and Connelly, R. E., Investigation of two-phase hydrogen flow in pump inlet line, NASA TN-D-5258 (1969).

10. Wright, B. M., Centrifugal pumping of liquefied gases, J. Sci. Instruments $\underline{44}$, 469-470 (1967).

11. Stepanoff, A. J., Centrifugal and Axial Flow Pumps, 2 Ed. (Wiley and Sons, New York, N.Y., 1957).

12. McCarty, R. D., Thermodynamic functions for helium 4 for temperatures from 2 to 1500 K with pressures to 100 MN/m^2 (1000 atmospheres), Nat. Bur. Stand. (U.S.), Tech. Note 631 (1972).

13. Cunningham, R. G., Hansen, A. G., and Na, T. Y., Jet pump cavitation, ASME Paper No. 69-WA/FE-29 (1969).

14. Wislicenus, G. F., Fluid Mechanics of Turbomachinery (McGraw-Hill, New York, N.Y., 1947).

15. Kovats, A., Design and Performance of Centrifugal and Axial Flow Pumps and Compressors (Pergamon Press, New York, N. Y., 1964).

16. Lazarkiewicz, S., and Troskolanski, A. T., Impeller Pumps (Pergamon Press, New York, N.Y., 1965).

17. Bird, R., Stewart, W. E., and Lightfoot, E. N., Transport Phenomena (Wiley & Sons, New York, N.Y., 1960).

18. Schlichting, H., Boundary Layer Theory, 4th Ed. (McGraw Hill, New York, N.Y., 1960).

19. DiStefano, J. F., and Caine, G. H., Cavitating characteristics of tank mounted cryogenic pumps and their predicted performance under reduced gravity, PESCO report (1961).

20. Jacobs, R. B., Martin, L. B., Hardy, R. J., Direct measurement of net positive suction head, J. of Basic Engineering 81, 47-152 (1958).

21. Ruggeri, R. S., and Moore, R. D., Method for prediction of pump cavitation performance for various liquids, liquid temperatures and rotative speeds, NASA Tech. Note D-5292 (1969).

22. Wright, M. K., Design comments and experimental results for cavitation-resistant inducers up to 40,000 suction specific speed, J. of Engineering for Power 86, 176-180 (1964).

23. Bulletins C-5246, C-5166, and C-5126, Globe Industries, Inc., 2275 Stanley Avenue, Dayton, Ohio 45404 (1967).

24. Apfel, R. E., The tensile strengths of liquids, Scientific American 227, No. 6, 58-71 (1972).

25. Finch, R. D., Kagiwada, R., Barmatz, M., and Rudnick, I., Cavitation in liquid helium, Phys. Rev. 134, No. 6A, 1425-1428 (1964).

26. Jacobs, R. B., Single phase transfer of liquefied gases, NBS Circular 596 (1958).

27. Schoch, K. F., Superconducting cryogenic motors, Book, Advances in Cryogenic Engineering 6, Ed. K. D. Timmerhaus, pp. 65-72 (Plenum Press, New York, N. Y., 1961).

28. Redmond, J. H., and Bott, F. W., Design study of a. c. motors to operate in helium from liquid to gaseous state, J. Spacecraft 5, No. 9, 1065-1069 (1968).

29. Johnston, H. L., Liquid Hydrogen: Propellant for aircraft and rockets, Final Report, Ohio State Research Foundation, Columbus 10, Ohio (1946).

30. Johnston, H. L., Liquid Hydrogen: Propellant for aircraft and rockets, Second Summary Report, Ohio State Research Foundation, Columbus 10, Ohio (1947).

31. Gottzmann, C. F., High pressure liquid-hydrogen and helium pumps, Book, Advances in Cryogenic Engineering 5, Ed. K. D. Timmerhaus, pp. 289-298 (Plenum Press, New York, N. Y., 1960).

32. Yonemitsu, H., and Okada, J., Spot-cooling with a cryogenic
pump. Book: Adv. in Cryogenic Engineering 9,
Ed. K. D. Timmerhaus, pp. 507-512 (Plenum Press,
New York, N. Y., 1964).

33. Darrel, B., and Schoch, K., An electrically pumped liquid
helium transfer system, Book, Adv. in Cryogenic
Engineering 11, Ed. K. D. Timmerhaus, pp. 607-611
(Plenum Press, New York, N. Y., 1966).

34. Kolm, H. H., Leupold, M. J., and Hay, R. D., Heat transfer
by the circulation of supercritical helium, Book,
Advances in Cryogenic Engineering 11, Ed. K. D.
Timmerhaus, 530-535 (Plenum Press, New York,
N. Y., 1966).

35. Mulder, I. J., A cold transfer system (Proc. 2nd Int.
Cryogenic Conf. Brighton, U. K., 50, 1968).

36. Wagner, W., An electrically driven pump and stirring unit
for use at low temperatures and high pressures,
Kaltetechnik-Klimatisierung 22, No. 10, 342-344,
In German, English translation by A. W. Beffie (1970).

37. Mark, J. W., and Pierce, W. B., Hydrogen targets at SLAC,
SLAC-PUB-883, Stanford Linear Accelerator Center,
Stanford University 94305 (1971).

38. Meservey, R., Superfluid flow in a venturi tube, Phys. of
Fluids 8, No. 7, 1209-1212 (1965).

39. Gelder, T. F., Ruggeri, R. S., Moore, R. D., Cavitation
similarity considerations based on measured pressure
and temperature depressions in cavitated regions of
freon-114, NASA TN D-3509 (1966).

40. Arp, V., Ballinger, E. R., Giarratano, P. J., and others, Helium heat transfer, Unpublished NBS Report (1972).

41. ASME Power Test Code, Chapter 4, Flow Measurement (Am. Soc. of Mech. Eng., New York, N. Y., 1959).

42. Hord, J., Anderson, L. M., and Hall, W. J., Cavitation in liquid cryogens I, NASA CR - 2054 (1972).

43. Moore, R. D., and Meng, P. R., Comparison of noncavitating and cavitation performance for 78°, 80.6°, and 84° helical inducers operated in hydrogen, NASA TN D-6361 (1971).

44. Pump Manual, prepared by the sub-committee on pumps of the equipment testing procedures committee. (Am. Inst. of Chem. Engineers, 345 E. 47th St., New York, N. Y. 10017, 1960).

45. Peck, J. F., Design of centrifugal pumps with computer aid, Proc. of Inst. of Mech. Eng. 183, Part 1, No. 17, 321-351 (1968-1969).

46. Arp, V., Forced flow, single-phase helium cooling systems, Book, Advances in Cryogenic Engineering 17, Ed. K. Timmerhaus, pp. 342-351 (Plenum Press, New York, N. Y., 1972).

47. Donnelly, R. J., Experimental Superfluidity (University of Chicago Press, Chicago, Ill., 1967).

48. Wilks, J., The Properties of Liquid and Solid Helium (Clarendon Press, Oxford, 1967).

49. Wood, G. M., Visual cavitation studies of mixed flow pump impellers, J. of Basic Eng., 85, 17-28 (1963).

DOCUMENT CONTROL DATA - R & D

(Security classification of title, body of abstract and indexing annotation must be entered when the overall report is classified)

1. ORIGINATING ACTIVITY *(Corporate author)*	2a. REPORT SECURITY CLASSIFICATION
Cryogenics Division National Bureau of Standards	unclassified
	2b. GROUP

3. REPORT TITLE

LIQUID HELIUM PUMPS

4. DESCRIPTIVE NOTES *(Type of report and inclusive dates)*
Summary report covering 5/72 through 12/72.

5. AUTHOR(S) *(First name, middle initial, last name)*

Philip M. McConnell

6. REPORT DATE	7a. TOTAL NO. OF PAGES	7b. NO. OF REFS
June 1973	81	49

8a. CONTRACT OR GRANT NO. MIPR FY 14557200411	9a. ORIGINATOR'S REPORT NUMBER(S) NBSIR 73-316
b. PROJECT NO.	
c.	9b. OTHER REPORT NO(S) *(Any other numbers that may be assigned this report)* AFAPL-TR-73-72
d.	

10. DISTRIBUTION STATEMENT

Approved for public release; distribution unlimited.

11. SUPPLEMENTARY NOTES	12. SPONSORING MILITARY ACTIVITY Air Force Aero-Propulsion lab. Air Force Systems Command Wright-Patterson Air Force Base, Ohio

13. ABSTRACT

This report summarizes studies of pump characteristics and performance in supercritical, normally boiling, and superfluid helium, and also presents results on a survey of commercially available pumps for helium service. Experimental measurements were made on a centrifugal pump which produced a maximum head of about 15 meters, and a maximum flow of about 2.5×10^{-4} m^3/s. Performance agreed approximately with classical affinity laws, but cavitation appeared to provide less of a performance limitation than expected. The survey turned up several pumps which have been used in helium, though relevant performance data is lacking.

DD FORM 1 NOV 65 **1473**

14. KEY WORDS	LINK A		LINK B		LINK C	
	ROLE	WT	ROLE	WT	ROLE	WT
Cavitation; helium; pumps; pump performance; superfluid.						

U.S. DEPT. OF COMM. BIBLIOGRAPHIC DATA SHEET	1. PUBLICATION OR REPORT NO. NBSIR 73-316	2. Gov't Accession No.	3. Recipient's Accession No.

4. TITLE AND SUBTITLE LIQUID HELIUM PUMPS	5. Publication Date June 1973
	6. Performing Organization Code

7. AUTHOR(S) Philip M. McConnell † † Present affiliation: Todd Research and Technical Div.,	8. Performing Organization

9. PERFORMING ORGANIZATION NAME AND ADDRESS Galveston, Texas NATIONAL BUREAU OF STANDARDS , Boulder Labs DEPARTMENT OF COMMERCE Boulder, Colorado 80302	10. Project/Task/Work Unit No. 2750459
	11. Contract/Grant No. MIPR FY14557200411

12. Sponsoring Organization Name and Address Aero-Propulsion Laboratory Wright-Patterson AFB, Ohio 45433	13. Type of Report & Period Covered Interim May - December 1972
	14. Sponsoring Agency Code

15. SUPPLEMENTARY NOTES

16. ABSTRACT (A 200-word or less factual summary of most significant information. If document includes a significant bibliography or literature survey, mention it here.)

This report summarizes studies of pump characteristics and performance in supercritical, normally boiling, and superfluid helium, and also presents results on a survey of commercially available pumps for helium service. Experimental measurements were made on a centrifugal pump which produced a maximum head of about 15 meters and a maximum flow of about $2.5 \times 10^{-4} \ m^3/s$. Performance agreed approximately with classical affinity laws, but cavitation appeared to provide less of a performance limitation than expected. The survey turned up several pumps which have been used in helium, though relevant performance data is lacking.

17. KEY WORDS (Alphabetical order, separated by semicolons)
Cavitation; helium; pump performance; pumps; superfluid.

18. AVAILABILITY STATEMENT [X] UNLIMITED.	19. SECURITY CLASS (THIS REPORT) UNCLASSIFIED	21. NO. OF PAGES
[ ] FOR OFFICIAL DISTRIBUTION. DO NOT RELEASE TO NTIS.	20. SECURITY CLASS (THIS PAGE) UNCLASSIFIED	22. Price